



Universidad Internacional de la Rioja
(UNIR)

Escuela Superior de Ingeniería y Tecnología

Máster Ingeniería Matemática y Computación

Scalar wave absorption by thin shell wormholes.

Master's Thesis

presented by: José María Sirvent

Directed by: Dr Gonzalo J. Olmo Alba y Dr Marc Jorba Cuscó

City: Jijona

Date: February 13, 2022

Ohne Musik wäre das Leben ein Irrtum.

(“Without music, life would be a mistake.”)

Friedrich Wilhelm Nietzsche

Index of contents

Abstract	vi
1 Introduction	1
2 Context and State of the Art	3
2.1 LIGO and VIRGO	3
2.1.1 LISA	6
2.2 Black holes	8
2.3 Wormholes	10
2.4 Current technical limitations	10
2.5 From Ancient Greece to Sgr A^*	12
2.5.1 Achilles and the tortoise	12
2.5.2 Basic strokes of Einstein's ideas	14
2.5.3 Teacher-student synergy: Minkowski-Einstein	16
2.6 Exact solution to Einstein's equations	17
2.6.1 Sgr A^*	19
2.7 State of the art	20
3 Objectives	22
4 Development of work	23
4.1 Numerov	24
4.2 Algorithm Proof: 1-Dimensional Schrödinger Equation	25
4.3 Approximation to our real problem	28

4.3.1	Absorption of scalar waves in the case of the Schwarzschild black hole	28
4.3.2	Embracing GSL and leaving Numerov	29
4.3.3	Crumbs on the road	34
4.4	Black Bounce: Going from a Schwarzschild BH to a WH.	36
4.5	Scalar wave absorption by thin-membrane wormholes	44
4.5.1	Hypergeometric	46
4.5.2	WolframEngine & Jupyter	47
5	Conclusions and Future Work	50
6	Glosario	59
A	Appendices	60
A.1	Source code	60

Index of Illustrations

2.1	Source:www.ligo.org - two stars colliding	3
2.2	Source: Veritasium6 - gravitational waves traveling	4
2.3	Source: Veritasium - gravitational waves reach Earth	5
2.4	Source: Veritasium - Hanford Site's LIGO	5
2.5	Source: Veritasium - Interferometer	6
2.6	Source: Veritasium - 2 LIGOs	7
2.7	Source: Veritasium - gravitational wave detection	7
2.8	Source: Wikepedia.org	8
2.9	Ground escape velocity	9
2.10	Source nasa.gov - Black hole	10
2.11	Double shadow wormhole [29]	11
2.12	Source: wikipedia.org - Zeno's paradox	12
2.13	Capacitor voltage	14
2.14	Tortoise coordinates	18
2.15	Source: wikipedia.org - Sgr A*	19
2.16	Source: www.huffpost.com - Interstellar	21
4.1	Wave equation	26
4.2	Coeficientes R y T	30
4.3	$\log_{10} 1 - R - T $	32
4.4	Partial absorption of the cross section with respect to frequency	33
4.5	V(x)	34
4.6	V(x)	35
4.7	Turtle coordinates	36

4.8	Waves and potential	36
4.9	$V(x)$	37
4.10	$R & T$	38
4.11	$\log_{10} 1 - R - T $	38
4.12	σ_l	39
4.13	$R & T$ coefficients	40
4.14	$\log_{10} 1 - R - T $	40
4.15	σ_l	41
4.16	Turtle	41
4.17	Wave and potential	42
4.18	$V(x)$	42
4.19	$R & T$	43
4.20	σ_l	43
4.21	σ_l	44
4.22	σ_l	45
4.23	Tortuga	47
4.24	V_{eff}	48
4.25	Coeficientes R y T	48

Abstract

This Master's Thesis has developed a series of programs that allow the theoretical characterization of different extremely compact objects through the absorption spectrum of scalar massless fields. Here specifically we've studied the differences between black holes and two wormholes types. For them, different numerical methods have been used, such as: Runge-Kutta Prince-Dormand, method in Nordsieck form by means of backward differentiation formula of several steps and Gaussian hypergeometric functions. In the development of these programs, C and libraries such as GSL, GMP and GLib have been used mainly. The graphs have been obtained using gnuplot and the graphical interface has been implemented using Tcl. A small portion of the code is written using Wolfram via Jupyter.

Thanks to this study, a black hole can be exactly differentiated from a wormhole since their absorption spectra are different. This could lead to discarding certain models or ideas about gravitation in the future.

Key words: Compact astrophysical objects; black holes; worm holes; Einstein-Rosen Bridge; Scalar wave absorption; Numerov algorithm; coordinated turtle; Gaussian hypergeometric functions.

Chapter 1

Attention

This is a machine translation If you're in doubt, please refer to the original Spanish document.

Chapter 2

Introduction

Gravitational wave astronomy is a reality that has been possible thanks to technological advances that the LIGO and VIRGO observatories have carried out over the last thirty years. detections current [1, 2] reveal the existence of very compact objects whose observational characteristics are compatible with the black holes predicted by general relativity. However, the current accuracy of these and other electromagnetic type observations (Event Horizon Telescope) [3] are not enough to rule out other possible types of compact objects. That is why there are currently great efforts theorists aimed at better understanding the observational signatures that other exotic objects might manifest [4].

One of the possible alternatives to black holes is found in wormholes [5], which would consist in compact structures of astrophysical size and non-Euclidean geometry capable of connecting distant regions of the universe. These objects would share astrophysical similarities with black holes (orbital properties) but they would be traversable, lacking an event horizon, which would distinguish them from these. In particular, both the shadows and wave absorption spectra of wormholes should be manifestly different from those of black holes.

In this Master's Thesis we will study the propagation of waves on geometries that are solutions of Einstein's equations of gravitation and from other theories such as black bounce geometries and that represent both black holes and wormholes. In particular, we will study the absorption spectra of scalar waves in different configurations (with and without electric charge). This will require solving differential

equations in partial derivatives of hyperbolic type in 3+1 dimensions, for which analytical tools (separation of variables, hypergeometric Gaussian functions) and numerical tools will be used.

In this work we will be able to reproduce some well-known results in the specialized literature on compact objects, thus showing that we have acquired solid knowledge and skill in the use of state-of-the-art numerical techniques. We will also face difficult technical problems that involve the combination of analytical and numerical methods. We do not always come to fruition in this fight, but the effort has rewarded us with many lessons learned and the desire to continue working on these issues.

The work is structured as follows: in the section 4.1 we become familiar with the Schrödinger equation and the Numerov method, as a simplified initial problem that will serve as the basis for attacking the following problems of increasing difficulty. Which will bring us to our final problem. In the section 4.3 we have already started to attack a real problem, a Schwarzschild black hole, which will allow us to develop all the necessary tools for the study of wave propagation on different geometries of wormholes. In the section 4.4 we will study a geometry similar to that used in the Schwarzschild black hole but that allows us to go from studying a black hole to a wormhole with the change of one parameter. Finally, in the section 4.5 we will study our final problem, a thin-membrane wormhole.

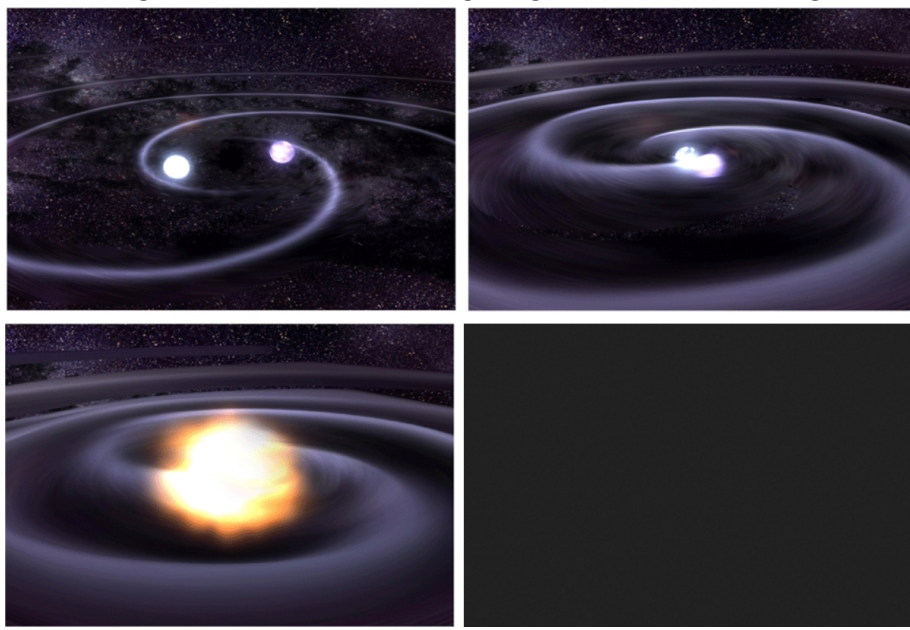
Chapter 3

Context and State of the Art

3.1 LIGO and VIRGO

LIGO 6 and VIRGO 6 are 2 interferometers located in the US and Europe that have made it possible to detect gravitational waves. Let's see what we're talking about.

Figure 3.1: Source:www.ligo.org - two stars colliding



As seen in the artistic representation Fig. 2.1 where we see two neutron stars rotating very close to finally collide, they create very intense gravitational waves that transport energy and information about the details of the collision throughout the space time.

Figure 3.2: Source: Veritasium6 - gravitational waves traveling



These gravitational waves travel throughout the universe as illustrated in Fig. 2.2. It should be noted that the signals that were detected in September 2015 and whose results were published in 2016 [8] had an energy equivalent to 50 times the energy of the entire visible universe. To put it in context, in 1/4 of a second, 3 solar masses were transformed into pure energy. To get an idea, the Sun produces enough energy in approximately 1s to cover our needs for the next 500,000 years, with the current demand of the planet. The Sun fuses about 600 million tons of hydrogen into helium every second, converting 4 million tons of matter into energy. That difference in mass, that is, we fuse 600 million tons of hydrogen that become 596 million tons of helium, is transformed according to Einstein's famous equation, $E = mc^2$, into energy. In this case, after the merger of the two black holes, of about 36 and 29 solar masses respectively, we obtained a black hole with a mass of 62 solar masses, with which the rest, 3 solar masses, was converted into energy in just a few thousandths of a second.

Gravitational waves stretch and compress spacetime as seen in this exaggerated artistic rendering Fig. 2.3.

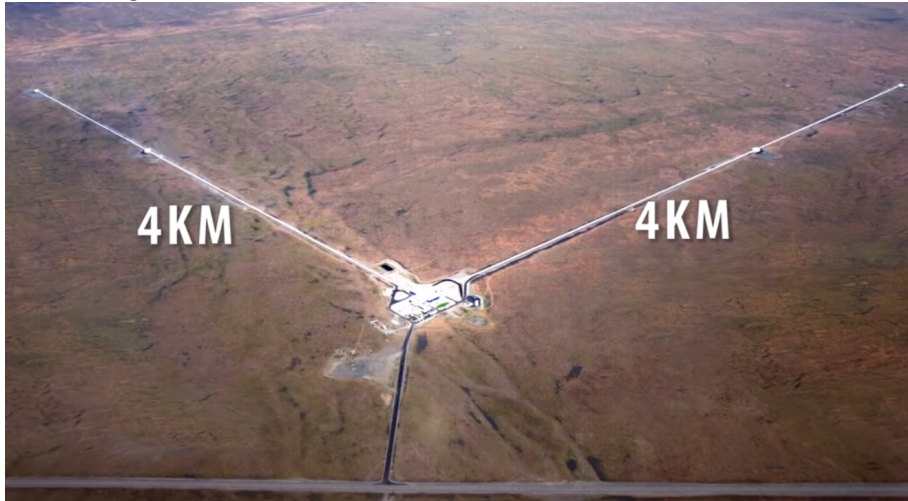
The waves, represented by a green waveform, create a distortion in spacetime of one part in 10^{21} or $10^{-21}m$, which is equal to the distance of one thousandth of the diameter of a proton



Figure 3.3: Source: Veritasium - gravitational waves reach Earth

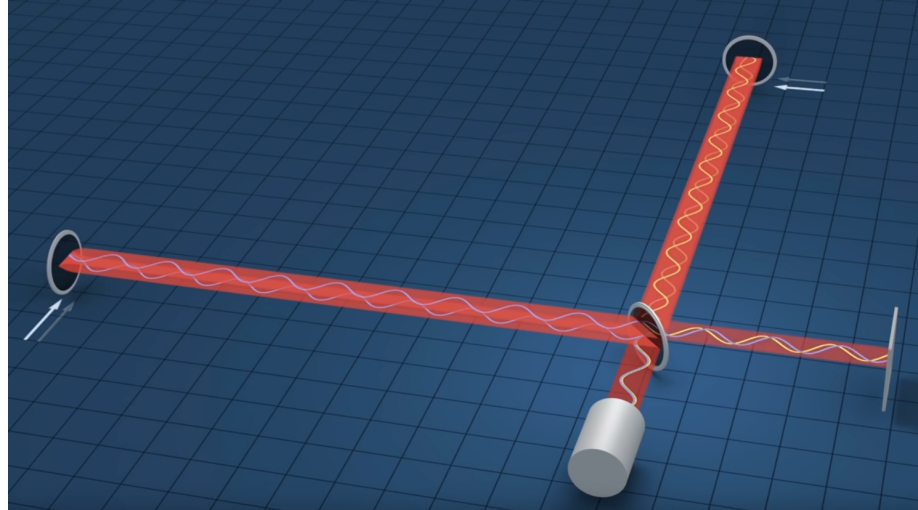
This is where the LIGO and VIRGO interferometers come into play.

Figure 3.4: Source: Veritasium - Hanford Site's LIGO



These interferometers Fig. 2.5 are huge due to the precision that needs to be achieved, but this is only part of the equation as a very precise and powerful laser is needed to detect these tiny variations. You need a laser that comes as close as possible to using one and only one wavelength because if the wavelength varies it will interfere with the measurement. If we imagine a ruler that varies its length by expanding and contracting, we see clearly that it will be impossible for us to give a measure of something. But we also need a large number of photons because the more photons the less uncertainty in the measurement, that's why this laser has

Figure 3.5: Source: Veritasium - Interferometer



1MW of power, added to this since we don't want anything to collide with the laser beam and interfere with it, it's in about vacuum tubes that take a whopping 40 days to reach a billionth of an atmosphere.

Now, if a gravitational wave expands / contracts everything, how can you measure an expansion contraction in spacetime? That is, if spacetime contracts, the laser will take less time and there will be no interference pattern. The key is that the laser travels 8km in a very short time while gravitational waves vibrate at around 100Hz. So, if a gravitational wave contracts spacetime, a quantum of light that we have sent out takes a certain time, but the one that came right behind when spacetime returns to its normal position, will take longer. This is where we will see the interference patterns.

Also, to be sure that this signal is not created by some kind of terrestrial noise, we have 2 LIGO Fig. 2.6 far enough apart that they will detect the signal almost instantly, since gravitational waves travel at the speed of the light. Having two or more detectors also helps to locate the origin of the emitting source.

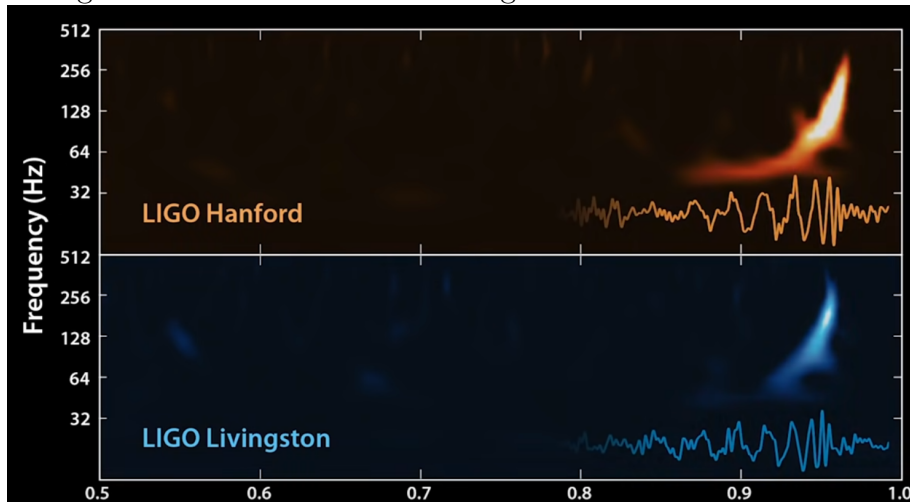
3.1.1 LISA

Simply to finish this section, point out the great interest that this field arouses. In 2017, LISA (Laser Interferometer Space Antenna) 6 was proposed as a candidate mission of the ESA (European Space Agency) 6. The mission is expected to run

Figure 3.6: Source: Veritasium - 2 LIGOs



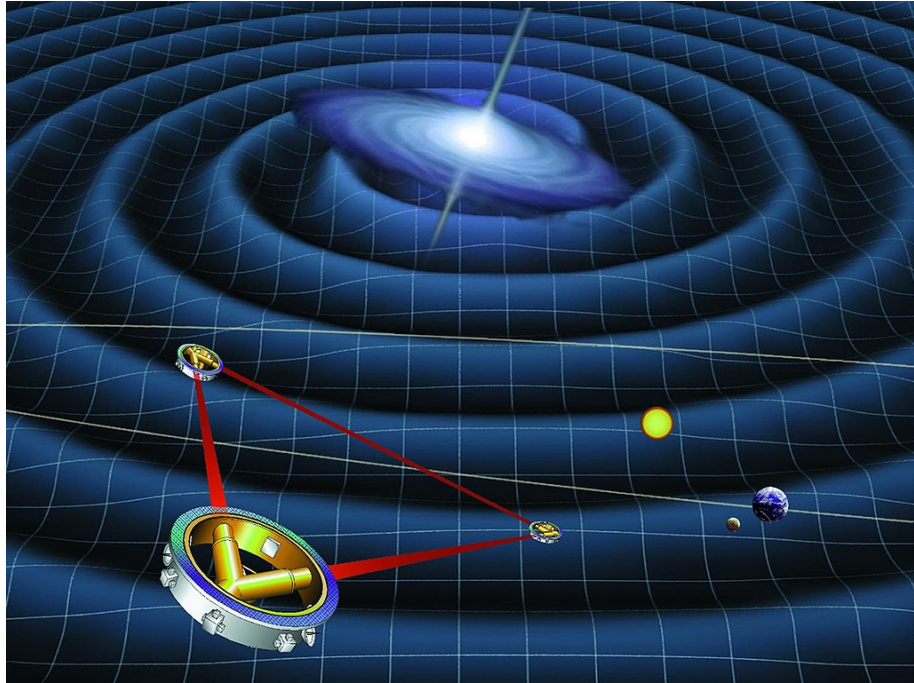
Figure 3.7: Source: Veritasium - gravitational wave detection



in the 1930s. LISA is a space interferometer with arms of a whopping 2.5 million km. Although it sounds like science fiction, the ESA has already set a date for its execution and also since 2015 there has been a mission, LISA Path Finder (LPF) 6 that is serving to test the technology necessary to carry out the project .

With this enormous interferometer it will be possible to detect collisions of super-massive black holes (with millions of times the mass of the Sun) that are impossible to detect by LIGO/VIRGO, since the frequencies of the fusion of this type of objects is very low and they need much longer arms.

Figure 3.8: Source: Wikipedia.org

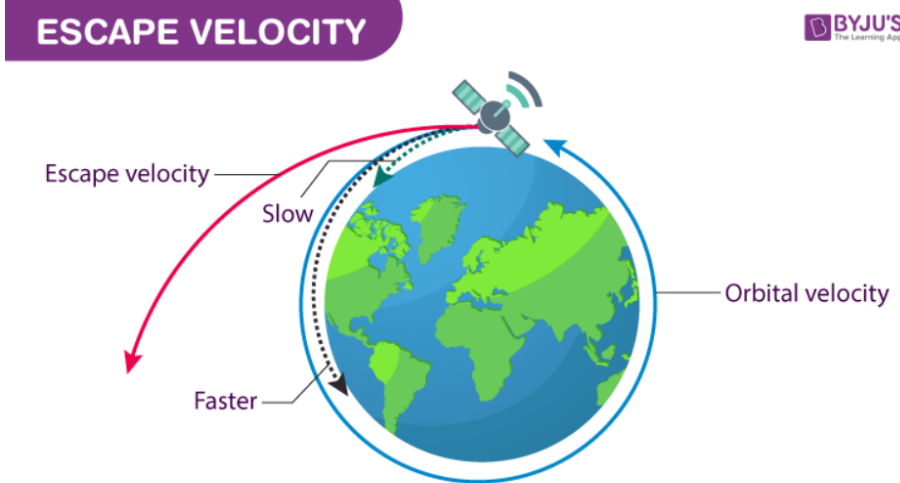


3.2 Black holes

What is a black hole or black hole (BH) 6? Gross modo, it is a region of spacetime resulting from a gravitational collapse caused by matter, where the gravitational attraction is so strong that not even light can escape. To get an idea let's imagine, using the notion of *escape velocity*, the experiment of throwing a stone. We will ignore the effect of air resistance and therefore the kinetic energy applied to the stone will be used entirely to convert it into potential energy with respect to the ground, that is, to climb a certain height. If we achieve a speed that exceeds the value $\sqrt[2]{\frac{2GM}{R}}$ where G is Newton's gravitational constant, M and R are the mass and radius of the Earth, we can escape from the Earth Fig. 2.9.

If we increase the ratio $\frac{M}{R}$ we could have an escape velocity that exceeds the speed of light and in this case not even light could escape, this is known as the Schwarzschild radius. In the case of the Earth, we would need to concentrate all its mass in something less than 1cm in radius. Here we could arrive at the image of a *black star* as John Michel did in 1784 and Pierre-Simon Laplace in 1799. However, at that time the speed of light was not a limit of nature as we now know but already we had the precursor idea of a black hole. The idea of a *black hole*

Figure 3.9: Ground escape velocity

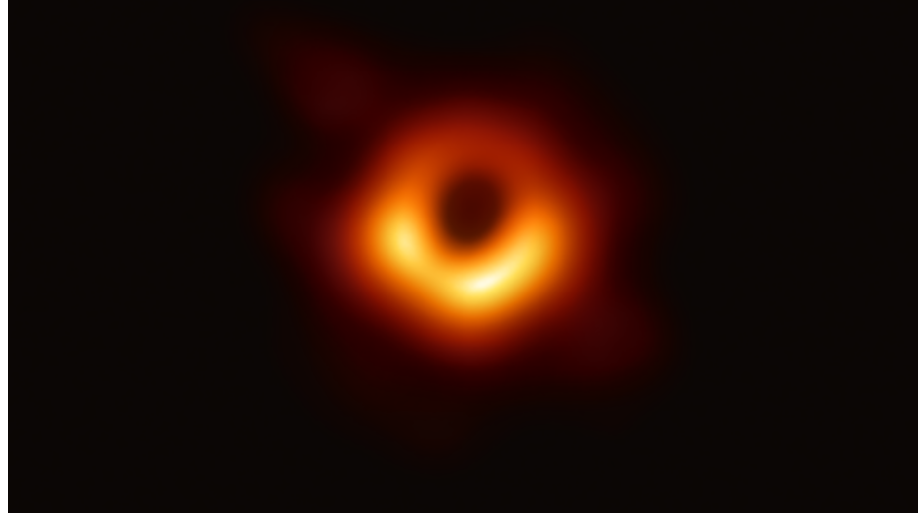
BYJU'S
The Learning App

comes when we encounter a sufficiently massive star that it has exhausted all of its available internal energy sources and cannot maintain enough pressure to prevent gravitational collapse. That mass is approximately $2M_{\odot}$ (that is, 2 times the mass of our Sun), a result obtained by Subrahmanyan Chandrasekhar in 1931. These objects collapse inwards, hence the term *black hole*. The Schwarzschild solution of Einstein's equation discovered in 1916 describes the gravitational field surrounding a body with spherical symmetry. The horizon occurs at a distance $r = \frac{2MG}{c^2}$ from the point of collapse. As we will see later when we study the Schwarzschild exact solutions to Einstein's equations, for this radius (taken in natural units where the universal constants equal 1) $r = 2M$, a mathematical singularity occurs. A singularity is a point at which a mathematical object is undefined or misbehaved in some particular respect. Therefore, we will not be able to continuously study the interior of that sphere.

But although black holes have an event horizon from which nothing can escape, they also have what is known as a photosphere. Fig. 2.10, which is a region in which photons are forced to orbit. Photons that approach the photosphere but manage to escape after a finite number of orbits are capable of reaching us and giving us evidence of the existence of this type of surface.

Still, the big problem with black holes is their space-time singularities [[14] [13]] that we don't know if they are a mathematical artifact or real. One of the possibilities

Figure 3.10: Source nasa.gov - Black hole



that eludes these singularities are wormholes or wormholes (WH) 6 since they lack them.

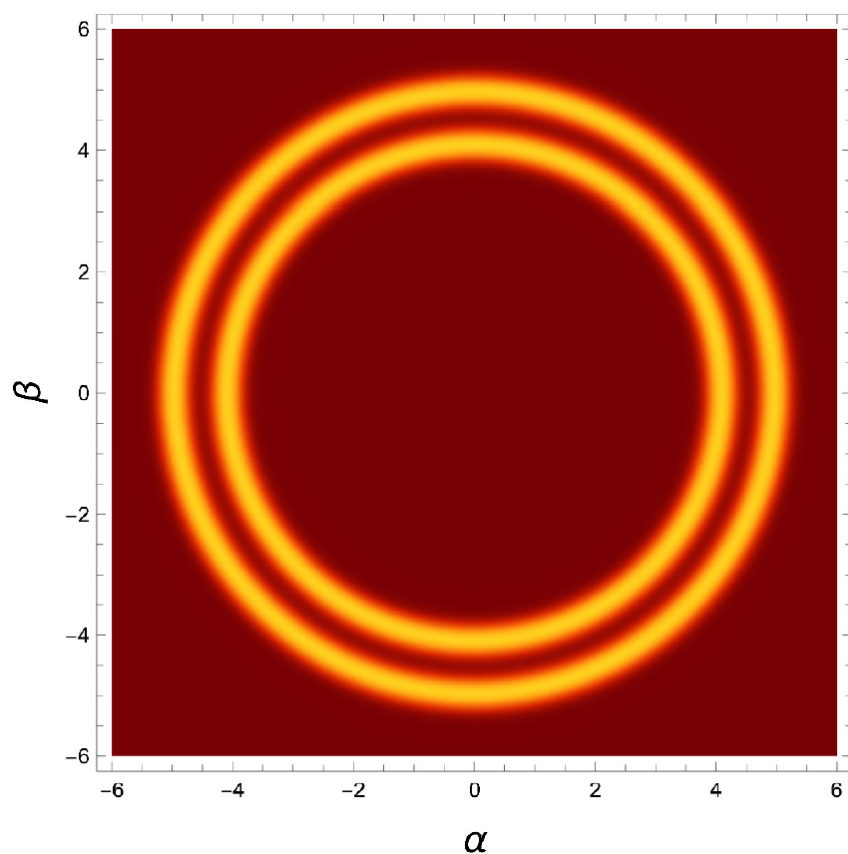
3.3 Wormholes

wormholes are what we could say a spatio-temporal connection between a black hole (which swallows everything down its throat) and a white hole (which expels everything that the black hole on the other side has swallowed) in which we connect two space-time points. These holes are known as Einstein-Rosen [6] bridges and you can travel instantaneously across them. A notable distinction between black holes and wormholes is that they lack an event horizon, so waves and information can flow in both directions. Consequently, both the shadows and the wave absorption spectra must be different. For example, in Fig. 2.11 we can observe the double shadow of a wormhole from one of its sides [7], where α and β are celestial coordinates.

3.4 Current technical limitations

Currently, thanks to the LIGO and VIRGO observatories, very compact objects have been detected whose characteristics are compatible with the black holes predicted by general relativity. However, the precision of these observations is not enough

Figure 3.11: Double shadow wormhole [29]

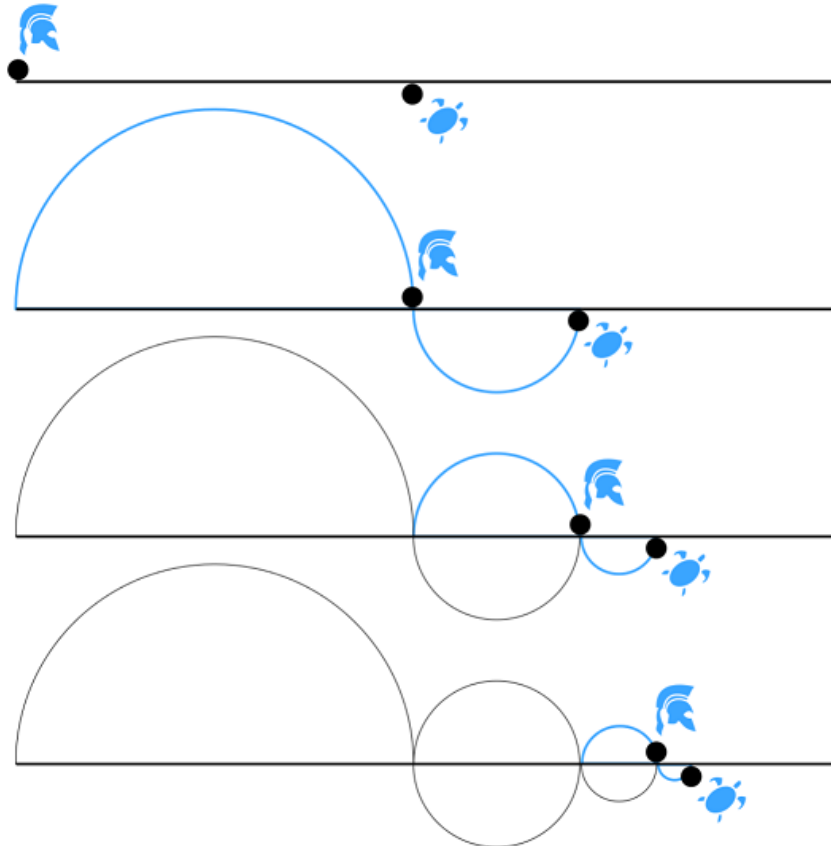


to rule out other types of compact objects. Something similar happens with the observation of shadows of black holes. It should be noted that the observation of gravitational waves or shadows compatible with the predictions of a black hole does not imply that other types of objects do not exist, so it is important to explore the characteristics of alternative objects that allow the observations to be correctly interpreted.

3.5 From Ancient Greece to Sgr A*

3.5.1 Achilles and the tortoise

Figure 3.12: Source: wikipedia.org - Zeno's paradox



One of Zeno's paradoxes, 490-430 BC, is about a race between the great Achilles, hero of the Trojan War, and a poor tortoise. According to Zeno, Achilles knowing of his superiority leaves the tortoise a certain distance advantage. Both opponents

have a constant finite speed. The race begins and when Achilles reaches where the tortoise was, the tortoise has traveled a small distance and the tortoise will still be ahead of Achilles. In the next instant of time, Achilles reaches the previous position where the tortoise was, but the tortoise has again traveled a small distance, so he continues to be ahead of the hero. If we extend this reasoning ad infinitum, Achilles will never catch the tortoise (at least apparently...) Fig. 2.12 The tortoise coordinates that we will use shortly take their name from this paradox.

Actually, an asymptote is being defined ¹. Let's do a thought experiment. We stand at a distance x from a door. In each step we will cover half of the distance that remains to reach the door. Now we wonder when will we reach the gate? The answer is never, since we will always be half the distance that separates us from the door, although we will be able to be as close to the door as we want. Putting it mathematically we have something like $d = (\frac{1}{2})^n$ which is only 0 as 'n' approaches infinity.

In real life, since no one has infinite time, we deal with this type of problem assuming certain types of simplifications and even knowing that the answer we give is not entirely correct, we assume it as such.

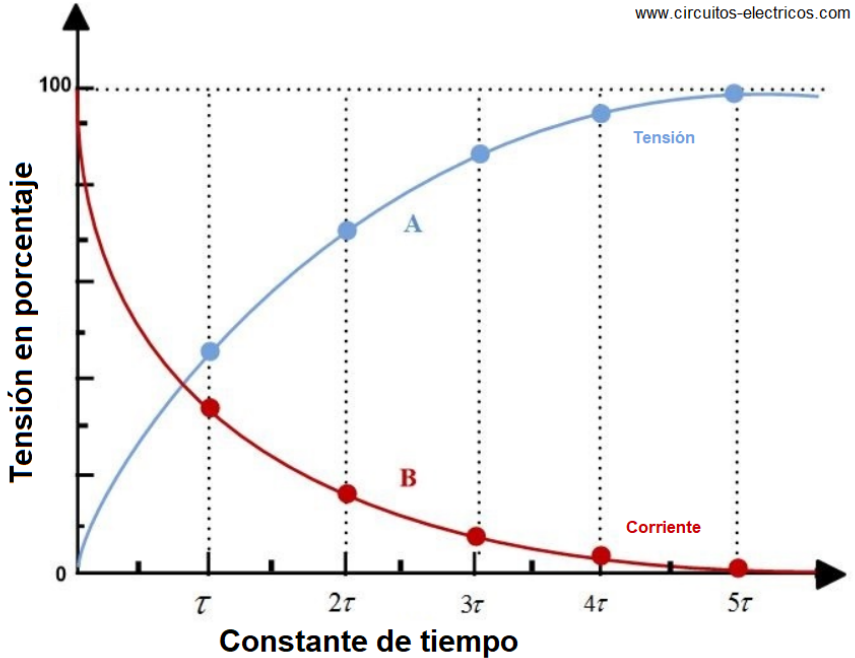
Perhaps one of the earliest examples of this in engineering school is the charge voltage of a capacitor Fig. 2.13. Knowing that the charging voltage has the form $v_c(t) = V(1 - e^{-\frac{t}{RC}})$ if we are asked when will the capacitor be charged? we usually say that when $t = 5\tau^2$ which equals a value of more than 99% of V. Actually, examining the equation we know that the answer $t = 5\tau$ is incorrect since $v_c(t)$ will be equal to V in infinite time, but the correct answer is of no interest because although it is correct for any configuration of the charging circuit we cannot wait an infinite time.

The important idea about turtle coordinates to remember is that the goal will never be reached since it is an asymptote.

¹Which in our case is perfect because asymptote means 'that does not fall'.

² 4τ is also very common and equals 98% of V

Figure 3.13: Capacitor voltage



3.5.2 Basic strokes of Einstein's ideas

For context, we are going to capture here some basic brushstrokes about Einstein's ideas about relativity and some tools that he used to implement his theories.

A concept that we are going to use a lot and very frequently in this MT is that of 'metric'. To measure lengths in infinitely small steps, we will need a ruler that measures the distance between infinitely close points. This rule for determining the measure of distances is called a metric. The most usual case is that of our school rule, which is the same with which we measure distances in Euclidean space, although taken to the limit this is only true in infinitely small domains since we will not find a surface as flat as the idea and definition flat. In fact, this exaggeration leads us to our next definition where this type of rule is of the Riemannian type and the geometry of such a space is called Riemannian, which is a Euclidean space in the infinitely small.

Another key idea that we are going to use frequently is that by differential geometry we know that the length of a curve does not depend on the given parameterization.

For the case of special relativity, in which gravitational fields are absent, the

natural metric is the so-called Minkowski metric, which we will explain in the next section.

Once at this point, Einstein thought that this geometric description should continue to be valid in the presence of a gravitational field, only that the Minkowski metric would have to be changed for another similar to a pseudo-Riemannian metric (it is not positive definite since it has the - 1 corresponding to the temporal coordinate) with the property that in each tangent space there exists a base $\{x_1, x_2, x_3, x_4\}$ whose scalar products could be represented by

$$g_{\mu\nu} = \begin{bmatrix} -1 & 0 & 0 & 0 \\ 0 & 1 & 0 & 0 \\ 0 & 0 & 1 & 0 \\ 0 & 0 & 0 & 1 \end{bmatrix}$$

The metric should be determined in some way by the matter that creates the gravitational field... but how? In classical mechanics it is known that the gravitational potential V originated by the matter of a continuum of density ρ , verifies the Poisson equation $\Delta V = 4\pi G\rho$, where G is the constant of universal gravitation and Δ is the Laplace operator $\partial^2/\partial x_1^2 + \partial^2/\partial x_2^2 + \partial^2/\partial x_3^2$, so There should be a similar law. Einstein thought that Poisson's equation should be replaced by a tensor equation of the form $G = \chi\tau^3$. Finally, and without going into details because this is already outside the purpose of this MT and does not enrich it either, Einstein realized that with the Ricci tensor R_{ab} the combination $R_{ab} - (1/2)Rg_{ab}$ plus a constant Λg_{ab} ⁴, which complies with a covariant type conservation law (known as the Bianchi identity). By matching this combination to the sources of matter, an equation is obtained that is consistent with the laws of conservation of matter and energy and that relates geometry with matter/energy:

$$R_{ab} - \frac{1}{2}Rg_{ab} - \Lambda g_{ab} = 8\pi GT_{ab},$$

³It is IMPORTANT to note that here G does not refer to the universal gravitational constant but to gravitational potentials

⁴Einstein added this constant to have a static model of the universe. It was not yet known that the universe is expanding and he himself denied it, calling it a big mistake. Today that constant is taken into account, although only for cosmology, where it is relevant.

which represents Einstein's (ten) equations of gravitation.

3.5.3 Teacher-student synergy: Minkowski-Einstein

In 1908 Minkowski⁵ realized that the special theory of relativity, described by his student Albert Einstein in 1905, could be better understood in a space 4-dimensional ($3 + 1$: the three spatial dimensions + 1 temporal). This idea of spacetime provided a fundamental point of view for the development of the new theory and would forever change our view of the world around us.

Minkowski spacetime is defined as

$$ds^2 = -dt^2 + dx_1^2 + dx_2^2 + dx_3^2; \quad (3.1)$$

which in polar coordinates is equivalent to $ds_M^2 = -dt^2 + dr^2 + r^2d\theta^2 + r^2\sin^2\theta d\varphi^2$, which we will also see in the form $ds_M^2 = \zeta_{\mu\nu}dx^\mu dx^\nu$ where

$$\zeta_{\mu\nu} = \begin{pmatrix} -1 & 0 & 0 & 0 \\ 0 & 1 & 0 & 0 \\ 0 & 0 & 1 & 0 \\ 0 & 0 & 0 & 1 \end{pmatrix}$$

The negative sign of ' dt^2 ' gives a formal expression for the radical difference between the time and space coordinates.

Starting from the 3D idea of differential arc length $ds^2 = dx^2 + dy^2 + dz^2$ and knowing from differential geometry that the length of the curve does not depend of the parameterization that is done, we change to polar coordinates $ds^2 = dr^2 + r^2d\theta^2 + r^2\sin^2\theta d\varphi^2$.

In 4D it would be $ds^2 = dx_1^2 + dx_2^2 + dx_3^2 + dx_4^2$ that we will usually see written as $ds^2 = g_{\mu\nu}dx^\mu dx^\nu$ using what is known as 'Einstein summation convention notation'.

Imagine that we have the following sum: $y = \sum_{i=1}^3 c_i x^i = c_1 x^1 + c_2 x^2 + c_3 x^3$ this is simplified using this convention: $y = c_i x^i$, as we see, the superscripts are not exponents but coordinate indices.

⁵Not only Einstein's teacher but also David Hilbert's friend

3.6 Exact solution to Einstein's equations

In December 1915 Karl Schwarzschild, while on the Russian front, obtains an exact solution where Einstein could ‘only’ find an approximate solution as indicated in ⁶ Einstein replies “... I had not expected that one could formulate the exact solution of the problem in such a simple way...”

The metric that Schwarzschild used is as follows

$$ds_{sch}^2 = - \left(1 - \frac{2M}{r}\right) dt^2 + \frac{1}{\left(1 - \frac{2M}{r}\right)} dr^2 + r^2 d\theta^2 + r^2 \sin^2 \theta d\varphi^2 \quad (3.2)$$

where $M \equiv \frac{GM}{c^3}$ y $r_s \equiv \frac{2GM}{c^3}$, staying $ds_M^2 = g_{\mu\nu} dx^\mu dx^\nu$ where now

$$g_{\mu\nu} = \begin{pmatrix} -\left(1 - \frac{r_s}{r}\right) & 0 & 0 & 0 \\ 0 & \frac{1}{\left(1 - \frac{r_s}{r}\right)} & 0 & 0 \\ 0 & 0 & r^2 & 0 \\ 0 & 0 & 0 & r^2 \sin^2 \theta \end{pmatrix}$$

with $dx^\mu = (dt, dr, d\theta, d\varphi)$. If we look at the equation 2.2 we see that we can take a common factor to $\left(1 - \frac{r_s}{r}\right)$ leaving the line element as

$$ds^2 = \left(1 - \frac{r_s}{r}\right) \left[-dt^2 + \frac{1}{\left(1 - \frac{r_s}{r}\right)^2} dr^2 \right] + r^2 d\Omega \quad (3.3)$$

We can integrate this same common factor that appears in the previous equation

2.3 $dr_*^2 = \frac{1}{\left(1 - \frac{r_s}{r}\right)^2} dr^2$, staying $r_* = r + 2M \ln \frac{r-2M}{2M}$, or

$$r_* = r + r_s \ln \frac{r - r_s}{r_s}, \quad (3.4)$$

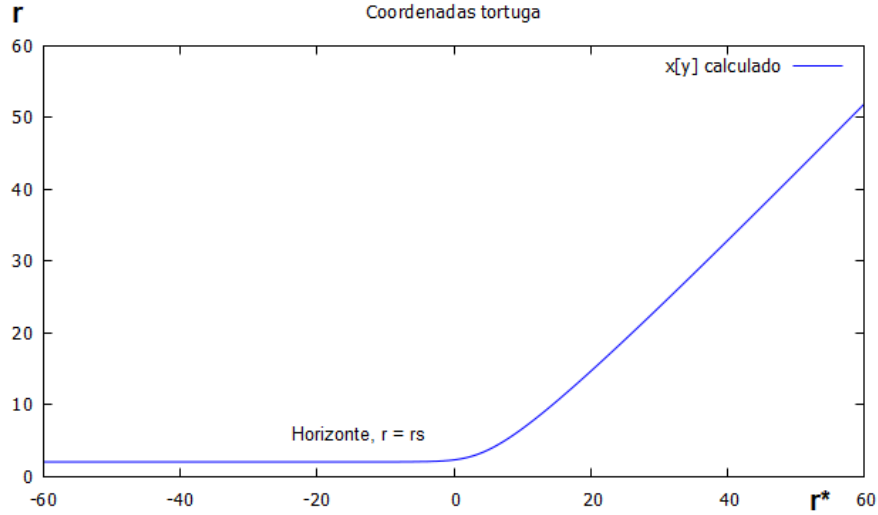
which is the usual expression for the tortoise coordinate ⁷. For a more complete reference on tortoise coordinates and other spherical spacetimes we can consult [19, 20, 21]. From here on it will be usual to refer to the tortoise coordinates as: y . So $r(r_*)$ will be expressed as xy or $x[y]$.

If we draw r with respect to r_* we have Fig.2.14

⁶Eisenstaedt, “The Early Interpretation of the Schwarzschild Solution,” in D. Howard and J. Stachel (eds), Einstein and the History of General Relativity: Einstein Studies, Vol. 1, pp. 213-234. Boston: Birkhauser, 1989.

⁷In English there is a different noun for land turtles, tortoise, and sea turtles, turtle. In our case the turtle race was on land so they are tortoise coordinates.

Figure 3.14: Tortoise coordinates



That if we analyze the equation 2.4 we see that it coincides with the intuitive idea. As r approaches r_s the $r_* \rightarrow -\infty$ times the logarithm. If $r > r_s$ and since r_s is very small then $r_* \approx r$. The exponential elbow, which in the figure is observed close to the value 0, is explained by defining $r = r_s + \Delta r$ and playing a bit we arrive at $r \approx r_s(1 + e^{\frac{r_* - r_s}{r_s}})$

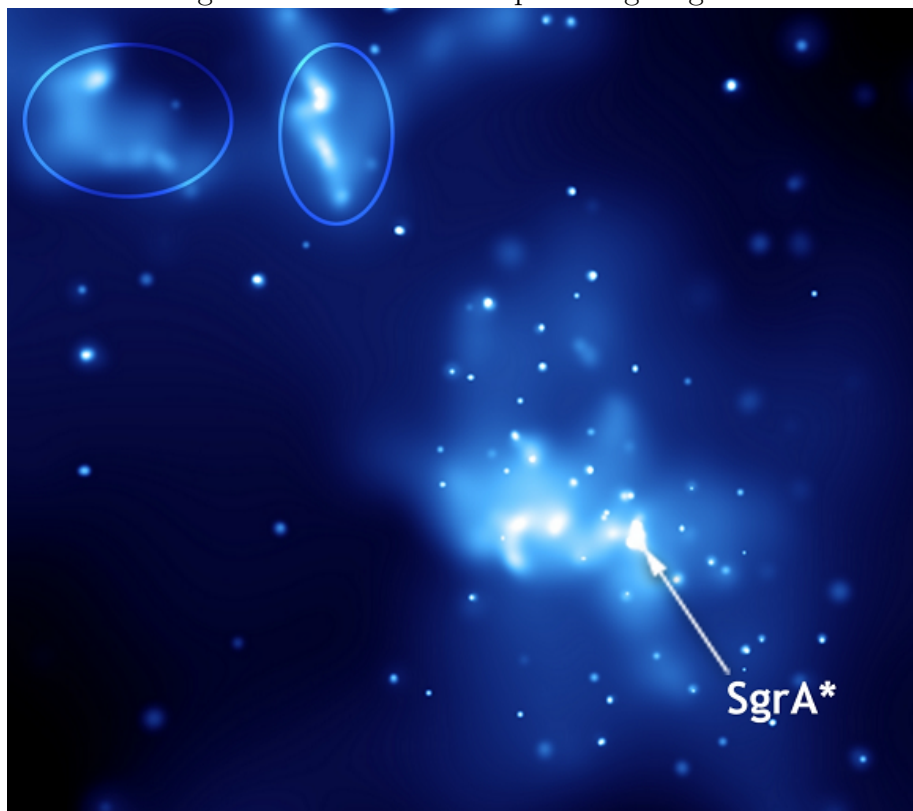
Looking at Fig. 2.14 we already have a clear reason for the name turtle coordinates. Coming from the right, $r_* > 0$, if we launch an object towards the black hole we would see how it approaches it and, upon reaching the event horizon, its speed decreases tending to zero when r tends to r_s , without being able cross the horizon, remaining ‘immobile’⁸ without actually touching the black hole since r never reaches to 0. This vision is due to the extreme red shift effect suffered by the light emitted by the object that approaches the horizon. For an external observer, the light emitted from the vicinity of the horizon takes an increasing time (asymptotically infinite as the horizon is reached) to reach him, which creates the illusion that said object never crosses the horizon.

⁸From outside the event horizon... because the object will be swallowed by the black hole mercilessly.

3.6.1 Sgr A*

We could not finish this introduction without talking about the possible black hole that rules our galaxy: Sgr A* or Sagittarius A* Fig. 2.15

Figure 3.15: Source: wikipedia.org - Sgr A*



In 2020 Reinhard Genzel and Andrea Ghez were awarded the Nobel Prize in Physics for the discovery of this supermassive object whose only explanation today is an ECO (Extreme / Exotic Compact Objects) 6.⁹

⁹It is thought to be a supermassive black hole, as it has millions of times the mass of our Sun

3.7 State of the art

The starting point of this MT is the article *Absorption by black hole remnants in metric-affine gravity* [9]. In it, it is emphasized that

Current observation capabilities are insufficient to confirm or rule out the existence of the BH event horizon. One of the interesting properties of wormholes is that they avoid BH singularities and also solutions are drawn naturally from the gravitational field. We will consider wormholes as ECO We can go further in their classification and subclassify them into UCOs (Ultra-Compact Objects)⁶ and ClePhOs (Clean Photonsphere Objects)⁶ Since ClePhos have an effective cavity between their surface and the photosphere we can characterize these by their absorption spectrum due to resonance.[9] (p.1 Introduction)

Another important article in the development of this MT is *Reissner-Nordström Black Holes in Extended Palatini Theories* [10] where we wanted to avoid the use of hypergeometrics by using approximations of these using equations (37-45) as a reference . We'll talk later about the problems I've had with hypergeometrics.

Finally, another key article has been *Shadows and optical appearance of black bounces illuminated by a thin accretion disk* [11] which has allowed me to study wormholes more easily thanks to using the line element from equation (2).

Perhaps the greatest effort to study and bring to the general public what a BH would look like and its event horizon was the movie Interstellar (2014). The article *Gravitational Lensing by Spinning Black Holes in Astrophysics, and in the Movie Interstellar*[12] discusses extensively the methods they used to represent as rigorously as possible this ECHO.

Since the electromagnetic observations of the event horizon seem extremely difficult to use in practice, the gravitational waves GW (Gravitational Waves) ⁶ can be used to study the structure of the BHs and their event horizon this is a path of study taken up in *Exotic Compact Objects and How to Quench their Ergoregion Instability*[15].

Figure 3.16: Source: www.huffpost.com - Interstellar

On the application of numerical methods in the characterization of ECOs, the article *Quasinormal modes of black holes and black branes*[16] is a very extensive review of the numerical methods used.

If we talk about code in solving similar problems we find *A public code for calculating the Hawking evaporation spectra of any black hole distribution*[17] where they also warn of the problems that have been found in the search for numerical solutions .

Our intention is to apply certain potentials to our model to obtain its behavior. For this we review publications that go along a similar line such as *General recursive solution for one dimensional quantum potentials: a simple tool for applied physics*[18], *Scattering and absorption of electromagnetic waves by a Schwarzschild black hole* [25] or *Resolution of the one-dimensional scattering problem by a finite element method*[26].

In general, I have found that the method used in the field is the Numerov method, so I have been reviewing where and how it has been used. A good example is found in *Numerov's Method for Approximating Solutions to Poisson's Equation*[27]

Also using Numerov's method for solving the Schrödinger equation we have *Practical points concerning the solution of the Schrödinger equation*[28].

Chapter 4

Objectives

The goal of this MT is to be able to characterize ECHOes by their absorption of massless scalar fields, as is done in our reference text [9], and to replicate their graphical results to allow us to distinguish between BH and WH. In particular, we need to be able to obtain the absorption spectrum of:

1. A Schwarzschild black hole
2. A wormhole using Black Bounce geometry
3. A thin membrane wormhole

Chapter 5

Development of work

Although all the code that we have written during the Master is done in Matlab, I have always had the feeling that it is difficult for other people to reproduce the numerical experiments. The first big problem is that Matlab is a paid software and although there are free alternatives like Octave or Scilab, surely the code is not 100% compatible, which represents a problem when others can check your results since the respective translations would have to be done. For this reason we have decided, even knowing that it is risky, to use some libraries and a language that is widely used in the scientific field such as: GSL (GNU Scientific Library) 6, GMP (GNU Multiple Precision Arithmetic Library) 6 and C.

Finally and out of my expectations, we will also use the Wolfram language 6 by using the free WolframEngine and Jupyter Python tool.

GSL is written in C, which is surely the most universal ‘high level’ language (that is, above languages such as assembly), we find it from tiny microcontrollers to mainframes. Furthermore, C is a high-performance language. We will use this library to be able to use different integration methods: Runge-Kutta (in different variables), Bulirsch-Stoer, Adams-Basforth / Adams-Moulton, Nordsieck, etc... Management of complex number and linear resolution systems such as: decomposition LU, QR decomposition, LQ decomposition, etc...

The use of GMP has been forced because the precision of a double is not enough to study a sufficiently large asymptotic region. In our case we have had to work with numbers with a precision of 130 bits. In fact, a posteriori it has become clear that

the use of the library does not really provide any interesting data that cannot be obtained through normal arithmetic, although the integration is carried out carefully.

Also in the field of C, we have used the GLib 6 library because we had to perform searches in ordered arrays and this library has a dichotomous search algorithm (among many more utilities).

For the graphs we are also going to use free software such as 6 Gnuplot, which is also used in the scientific field.

For the creation of a friendly graphical interface to carry out the numerical experiments, we have used the programming language Tcl 6 since very soon we have realized the immense need to be able to vary our parameters to do the experiments.

5.1 Numerov

This numerical method starts from the difference equation of order 2

$$\Delta_2 = \frac{u_{i+1} - 2u_i + u_{i-1}}{h^2} \quad (5.1)$$

and it is especially indicated for differential equations of the second degree that do not contain the first derivative. In general, we will express it as

$$[p(x)u'(x)]' + q(x)u(x) = s(x) \quad (5.2)$$

After applying 4.1 on the derivative of order 2 and 4 of the equation 4.2 we arrive at

$$u^{(4)}(x) = \frac{d^2}{dx^2}[-q(x)u(x) + s(x)]$$

than applying 4.1 again but this time on the right side we get

$$u^4 = \frac{(s_{i+1} - q_{i+1}u_{i+1}) - 2(s_i - q_iu_i) + (s_{i-1} - q_{i-1}u_{i-1})}{h^2}$$

that combining with the equation $\Delta_2 = (u_{i+1} - 2u_i + u_{i-1}/h^2 = u''_i + h^2u^{(4)}/12)$ y $u''_i = s_i - q_iu_i$ we obtain Numerov's algorithm of the form

$$c_{i+1}u_{i+1} + c_{i-1}u_{i-1} = c_iu_i + d_i + O(h^6)$$

with the corresponding coefficients

$$\begin{aligned} c_{i+1} &= 1 + \frac{h^2}{12} q_{i+1} \\ c_{i-1} &= 1 + \frac{h^2}{12} q_{i-1} \\ c_i &= 2 - \frac{5h^2}{6} q_i \\ d_i &= \frac{h^2}{12} (s_{i+1} + 10s_i + s_{i-1}) \end{aligned}$$

This method maintains terms of order h^4 by removing terms of order h^6 and higher. Therefore, this method is locally O(6)[28] but globally it is O(4), although this method is still preferred for solving the Schrödinger equation because in practice it has a higher performance than other algorithms in the same order since it has a larger periodicity interval [30].

5.2 Algorithm Proof: 1-Dimensional Schrödinger Equation

We are going to test our algorithm with a similar problem regarding the form of its differential equations: the 1-dimensional Schrödiger equation. For this we start from various papers, books and publications such as the explanations of chapter 3 of [22] where the Numerov method is explicitly used, the Revista Brasileira de Ensino de Physics [23] where the problem is explained more graphically and an example of computational physics where to discuss An Introduction to Computational Physics [24].

$$\phi''(x) + \frac{2m}{\hbar^2} [\epsilon - V(x)] \phi(x) = 0$$

from which we have the exact solution with the following potential

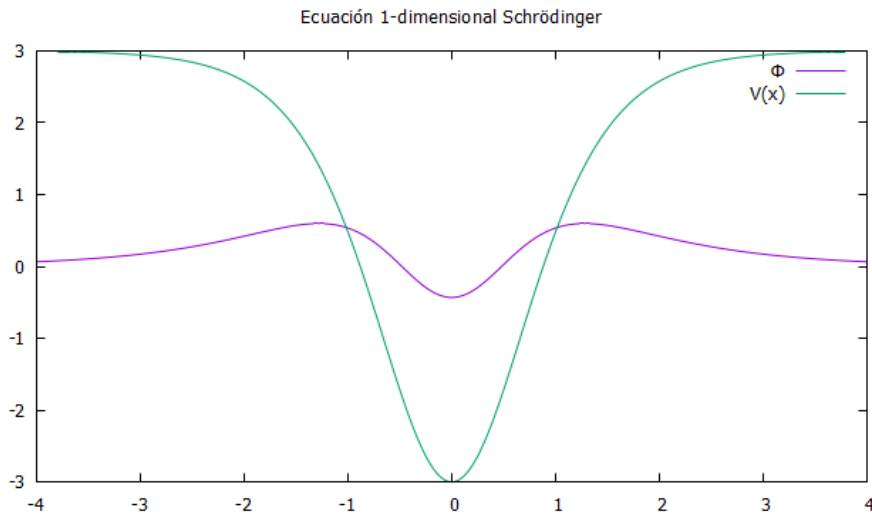
$$V(x) = \frac{\hbar^2}{2m} \alpha^2 \lambda(\lambda - 1) \left[\frac{1}{2} - \frac{1}{cosh^2(\alpha x)} \right]$$

and this energy

$$\epsilon_n = \frac{\hbar^2}{2m} \alpha^2 \left[\frac{\lambda(\lambda-1)}{2} - (\lambda-1-n)^2 \right]$$

If we draw the results obtained using as parameter values $\hbar = m = \alpha = 1, \lambda = 4, n = 2$ we see that the results obtained agree with those expected

Figure 5.1: Wave equation



To solve the equations we must take into account that in the physical system the wave function $\phi(x) \rightarrow 0$ when $|x| \rightarrow \infty$ so we can integrate from left to right or from right to left. Integration thus requires integrating from an exponentially increasing region, to an oscillatory region, and finally to an exponentially decreasing region.

The accumulated error will be significant if we integrate the solution from the oscillatory region towards the decaying exponential region. This is so because an exponentially increasing solution is a possible solution, which could bury the solution in the increasing errors of the integration method.

To avoid this risk, we obtain the solutions from both sides and join them in the region of the potential well. Usually the union is made when the potential starts to change and meets the energy level.

The joining region is adjusted so that the integrated solution on the right, $\phi_r(x_r)$, coincides with the integrated solution on the left, $\phi_l(x_l)$, and also the continuity conditions are satisfied, which in this case are

$$\phi_r(x_r) = \phi_l(x_l)$$

$$\phi'_r(x_r) = \phi'_l(x_l)$$

Combining both, we have

$$\frac{\phi_r(x_r)}{\phi'_r(x_r)} = \frac{\phi_l(x_l)}{\phi'_l(x_l)}$$

and using central differences

$$f(\epsilon) = \frac{[\phi_l(x_r + h) - \phi_l(x_r - h)] - [\phi_r(x_r + h) - \phi_r(x_r - h)]}{2h\phi(x_r)} = 0$$

Why have we used the time-independent Schrödinger equation to test Numvero's algorithm? The answer is that the solutions of the Schrödinger equation behave correctly only for certain values of energy. For very small values of U_0 , there is only one allowed energy. Therefore, if we obtain the expected results with the Numerov algorithm, we can be more than sure of its correct operation.

The code developed in C implements the Numerov method for the integration of the wave function, the secant method for obtaining the eigenvalues, the wave function, the 'f' function and the potential function we have to implement as well Simpson's method for function normalization.

The translation of the equations is surprisingly direct and the only thing that seems strange to me is the normalization of the wavefunction using Simpson's rule (also direct translation). In this first approximation, the code of the numerical methods has been done by hand, but the intention is to do it through GSL since it would give enormous flexibility.

Once the first results have been observed, the convenience of being able to carry out numerical experiments quickly, easily and efficiently has become obvious. Although the compilation of such a tiny program takes only a few seconds, it is clearly a cumbersome process. Our choice has been to create a graphical interface to simplify the process. Thus, every time you want to modify a parameter and see the result, it can be done easily and simply. This in turn enables anyone who doesn't want to use the interface the same functionality by changing the input data. The

graphical interface that we have made in Tcl 6 allows us to change variables of the numerical method, physical variables of the problem and some variables of the graph of the results.

5.3 Approximation to our real problem

5.3.1 Absorption of scalar waves in the case of the Schwarzschild black hole

In a first approximation to our problem we are going to see if we are able to plot the transverse absorption spectrum of massless scalar fields in the Schwarzschild case. For this, we have the reference of Fig.6 of [9]. The process is an iterative process in which we are going to calculate the reflection and transmission coefficients of equation 27 [9], $\phi(x) = R_{lm}e^{-iwr_*} + T_{lm}e^{iwr_*}$, where R (Reflection) and T (Transmission) are complex numbers. The equation we are going to solve is Equation 26 [9] reproduced here for convenience, $\left(\frac{\delta^2}{\delta r_*^2} + \omega^2 - V_\phi(r_*)\right)\phi(x, t) = 0$, which as we see is like our old well-known Schrödinger equation..

The first thing we will do is solve the following ODE:

$$\begin{cases} x'[y] = 1 - \frac{r_s}{x[y]} \\ x[y_L] = r_s(1 + e^{(y_L/r_s - 1)}) \end{cases}$$

We take advantage of the fact that this case is simple and we have the analytical expression for \mathbf{x} and \mathbf{y} .

$$x = r_s(1 + e^{(y_L/r_s - 1)})$$

$$y = x + r_s \ln(x/r_s - 1)$$

to see if our calculated values are correct.

Once the turtle coordinates are obtained, we can now calculate the effective potential

$$V_{eff} = \frac{l(1+l)(r_s - x[y])}{x[y]^3}$$

At this point we are ready to calculate the Reflection and Transmission coefficients. Our system of equations is the following:

$$\phi = \begin{cases} e^{ikx} + Re^{-iwr_*}, & x \rightarrow -\infty \\ Te^{iwr_*}, & x \rightarrow \infty \end{cases} \quad (5.3)$$

that dividing by the unknown factor T, we obtain the initial conditions:

The boundary conditions are given in equation 33 [9]

$$\phi = \begin{cases} e^{-iwr_*}, & x \rightarrow -\infty \\ e^{iwr_*}, & x \rightarrow \infty \end{cases}$$

And with them calculate the partial absorption of the cross section

$$\sigma_l = \pi(2l + 1)(1 - |Rw|^2)$$

5.3.2 Embracing GSL and leaving Numerov

To obtain the coefficients R and T of our system of equations that will allow us not only to check that the calculations are correct (since by definition $R + T = 1$) but also that they are essential to obtain the cross section of the partial absorption, σ_l , we need to work with: matrices, vectors, complex numbers, LU decompositions and numerical integration; We see that our implementation of Numerov is a hindrance since it is not adapted to the GSL API 6, which is the one that offers us all the facilities that I have just commented on plus an infinity more. In addition, as I commented in 4.1 finally the Numerov method has a global $O(4)$ and GSL 6 offers methods of up to $O(8)$ such as the Runge method -Kutta Prince-Dormand 6 but it also allows us to experiment with a wide range of algorithms¹.

For the resolution of the numerical integration of the different ODEs I have used the Runge-Kutta Prince-Dormand method (8, 9) but in reality I have not seen any difference in the calculation time or the shapes of the graphs with the classic Runge-Kutta -Fehlberg (4, 5).

The first thing we need to do is solve equation 36 of [31] which is given by its derivative and the initial condition at a point far away, $-\infty$ (in our case -150). Here,

¹see section: Ordinary Differential Equations, Stepping Functions

$x[y]$ are the turtle coordinates:

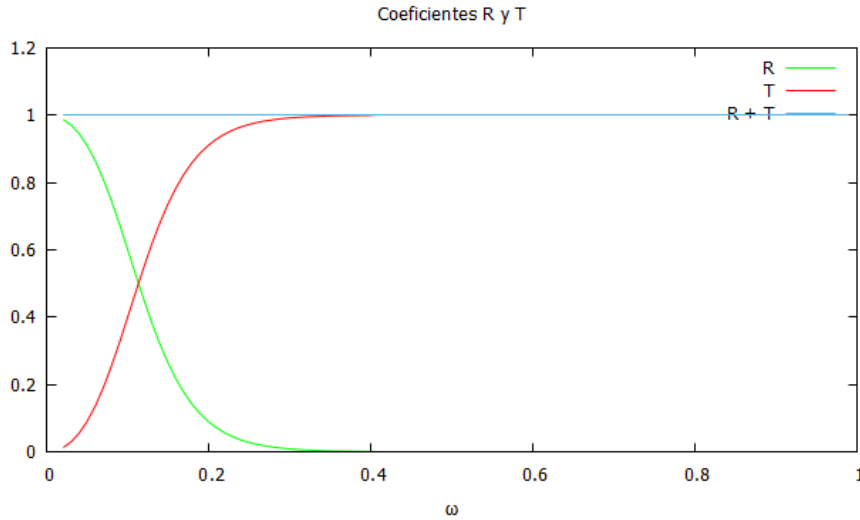
$$\begin{cases} x'[y] = 1 - \frac{r_s}{x[y]} \\ x[-\infty] = r_s(1 + e^{\frac{-\infty}{r_s}-1}) \end{cases}$$

Once we have obtained the value of $x[y]$ we can obtain the values of ‘q’ in the Sturm-Liouville function, $[p(x)u'(x)]' + q(x)u(x) = s(x)$.

$$q(x) = w^2 - \frac{l(1+l)(r_s - x[y])}{x[y]^3}$$

Now we can proceed to the backward integration of the Schrödinger equation with the form $\phi'' = (V(x) - w^2)u(x)$, which allows us to solve the system of equations 4.3 and obtain the coefficients R and T, where to obtain a curve we will vary the frequency w obtaining Fig. 4.2

Figure 5.2: Coeficientes R y T



As we can see, it is confirmed that the sum of both coefficients is equal to unity.

Perhaps we have missed a very significant aspect of this simple graph. As we can see, at low frequencies we have that the reflection coefficient, R, is different from 0. That is: the waves that we send to the black hole are reflected. Therefore, a black hole does not absorb everything. How a black hole absorbs a wave depends on the frequency/wavelength of the wave. If the frequency is very high (wavelength much smaller than the horizon size) then the wave is completely absorbed and the absorption cross section is constant (does not change with frequency). On the other

hand, for much longer wavelengths, the absorption will be minimal. For wavelengths the size of the horizon, oscillations will be observed, as we will see shortly. And it is this fact that will allow us to differentiate between different ECOs. In our case, we are interested in distinguishing a BH from a WH.

In general, there is an intuitive idea that a black hole completely absorbs everything, but this is not the case as we have just seen. Here, we can make a comparison with something that is much closer to us and known, such as radio waves and their reception according to orography. Our black hole will be the mountains around us, and the waves we send out are TV waves (which are over tens or hundreds of MHz) and AM radio waves (which are over tens or hundreds of kHz).

If we are locked in a valley, it will be highly likely that we will not be able to watch television unless there is a repeater nearby. In fact, the repeaters are placed at the top of the mountains so that they do not absorb the waves and to project them towards the valley. This is due to the fact that the high frequencies of the television signal are absorbed by the mountain, preventing its reception. On the other hand, with radio waves, especially AM, no repeater is necessary for the correct reception of the signal. AM waves have such a wavelength that they are able to 'go around' mountains and reach their destination. The mountains do not absorb them or do so in a small proportion.

If we examine the error of the value obtained in the sum of the coefficients R and T with its expected value, we obtain Fig. 4.3

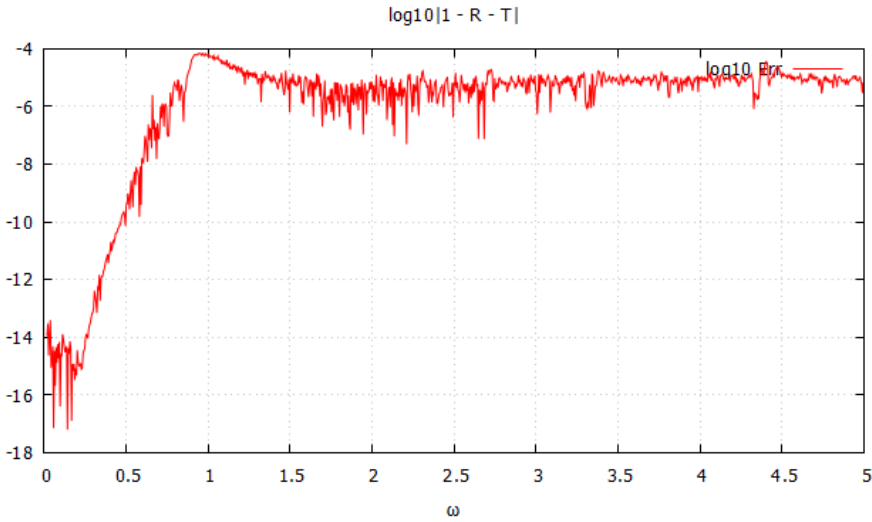
As we can see, it increases with frequency but stabilizes around the fifth decimal.

If we obtain graphs for different angular moments we obtain the following partial absorptions Fig. 4.4 para $l = 0, l = 1, l = 2, l = 3, l = 4$:

Which, as we see, agrees with the partial absorption graph of the cross section for a given angular momentum according to Fig. 6 of [9], having used equation 33:

$$\sigma_l = \frac{\pi}{\omega^2} (2l + 1).$$

To obtain the graph at such a far distance from the object of study, the GMP 6 library was used, as we will explain below, although the asymptotic region is actually around $[-60, 60]$ and the precision of the doubles is not enough for us as explained below.

Figure 5.3: $\log_{10}|1 - R - T|$ 

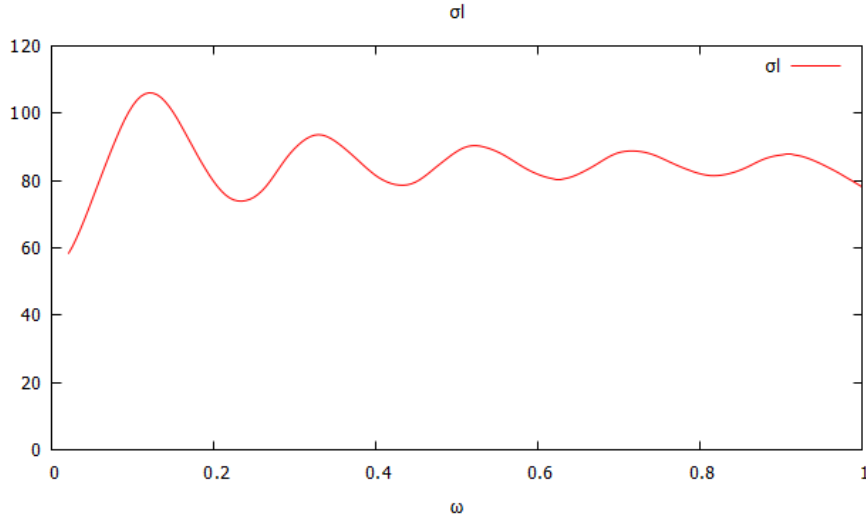
Expanding our asymptotic region

Until now we were working in the region $[-40, 40]$ and even $[-60, 60]$ but it was not ‘enough’ to fully see the asymptotic region, we are very close but we have to move a little further from our black hole . It is then, when trying to go to a region $[-150, 150]$ we have found that we no longer obtained any results. After a lot of research into why we got results in one region and not in another further away, we realized that at a certain distance the turtle coordinates, which are asymptotic, the standard floating point arithmetic was not enough... that is: we got to its resolution limit and all values were constant so the derivative was 0.

Since I wanted to go a bit further because I needed to expand the region to display the entire asymptotic region, we were forced to use a variable multiple precision library, GMP 6, which is the equivalent of vpa, variable-precision arithmetic, in Matlab.

With this new tool in hand, we were able to reach much further regions and with a range of $[-150, 150]$ the asymptotic region could already be seen to a large extent, but was this the only option? Unfortunately the answer is no. The time we spent to see why the program that worked well in ranges of $[-20, 20]$ or even $[-60, 60]$ but not for example $[-150, 150]$ was enormous. In the end we solved the problem using GMP but on the one hand the region $[-60, 60]$ is more than enough for the study

Figure 5.4: Partial absorption of the cross section with respect to frequency

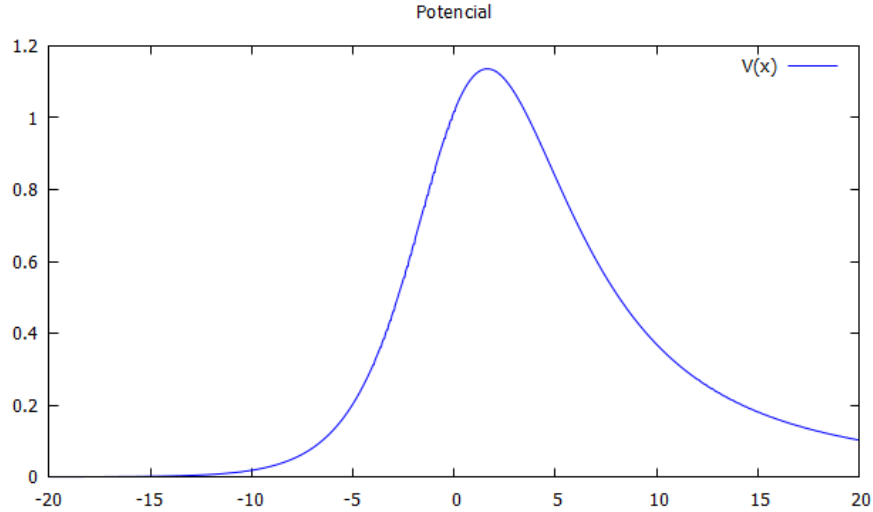


of σ_l and on the other hand the real problem was that I was integrating from the left from the asymptotic region where each of the points is practically the same and therefore the doubles do not manage to differentiate between them, when it could have integrated from the right where this problem does not exist.

Looking back, this has undoubtedly been our biggest mistake, although not everything has been wasted, since we have learned to use the GMP library, which is certainly a fantastic library, but since it makes everything a little more difficult, since the calculations are already complicated and even having created a wrapper for the use of GMP, the code is more obscure and difficult to understand. For this reason and because the results are totally correct we have not used the library again in the rest of the MT.

To get an idea of what we are talking about, I am going to show the potential in two study regions. In the first $[-20, 20]$ Fig. 4.5 we see that the potential does not reach 0 when we go towards $+\infty$, although it is really close.

If we go to the region of $[-60, 60]$ Fig. 4.9 things change and we can already say that we have an asymptotic region

Figure 5.5: $V(x)$ 

5.3.3 Crumbs on the road

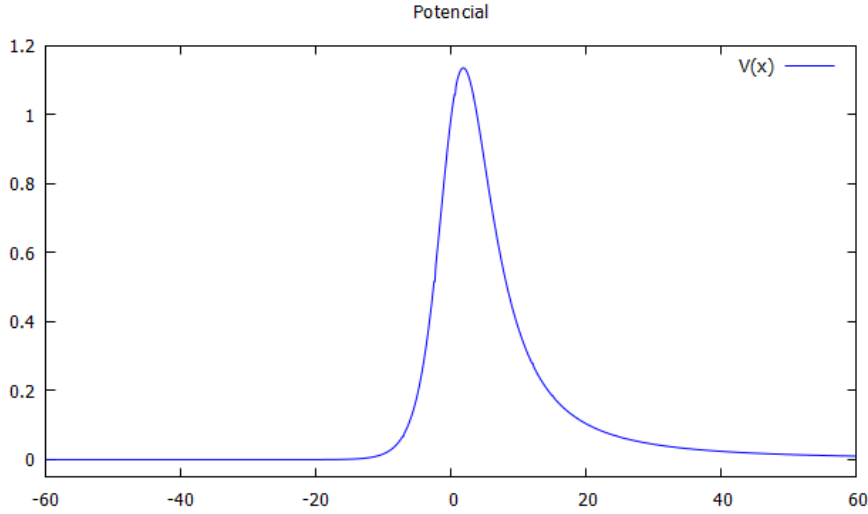
The Schwarzschild case has fulfilled the essential role of reference to be certain that we are on the right track when making our calculations. Let us remember that this matter is an **important point of physics that is still open** in which important efforts are certainly being made lately to better understand it. The fact that it is a world yet to be explored makes it even more attractive and is partly the reason why I chose this theme.

Somewhat related to this study of spacetime, it has recently been ‘verified’ in the laboratory² the actual existence of an Alcubierre engine [33] which basically consists of compressing spacetime in front of us, expanding it behind us to allow us to travel faster than the speed of light without breaking any physical law. A classic on the subject of space travel in spacetime through wormholes would be [34]. Therefore, what seems like science fiction to us today may not be so tomorrow (remember the great Jules Verne).

The first graph that we have to obtain are the turtle coordinates, and these must have a shape similar to that of Fig..4.7.

In fact, in this particular case we have, on the one hand, the calculated tur-

²<https://www.extremetech.com/extreme/329631-scientists-havent-created-a-warp-bubble-but-theyre-a-bit-closer-to-testing-one>

Figure 5.6: $V(x)$ 

tle coordinates, inverse analytics and inverse calculated coordinates. As we see the 3 coincide and therefore we know for sure that the result is correct. But the Schwarzschild case is the simplest and we are not going to be lucky enough to have an analytic expression for the tortoise coordinates.

The next step is to plot the transmitted and reflected waves along with the potential under study, as shown in Fig. 4.8.

As we can see, the interaction with the potential causes the phase difference between the real part and the imaginary part. We also see the interaction between the wave and the potential where this is not null. Finally we see how the wave is able to overcome the potential and be transmitted. The wave is sent from the left side in the direction of the right side. Therefore, on the left side we have the reflected wave and on the right side we have the transmitted wave.

For clarity and to be able to focus more on the potential, since it is an important part of the following calculations, we draw the potential only Fig. 4.9

Next we draw the coefficients R and T. The correction of these is key to reach the final point. By definition, $R + T = 1$ over the entire frequency range. That is, the sum of the reflected and transmitted wave is equal to the wave that we have sent Fig. 4.10.

We will also plot the error in the theoretical calculation of the coefficients as

Figure 5.7: Turtle coordinates

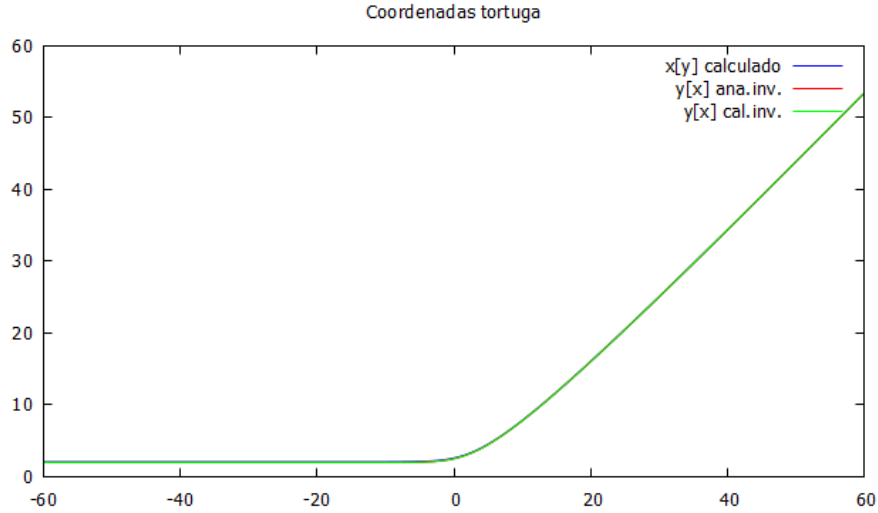
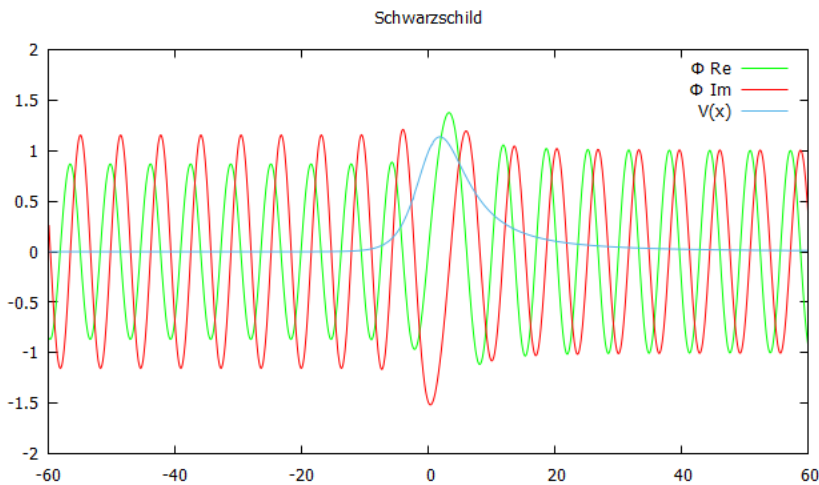


Figure 5.8: Waves and potential

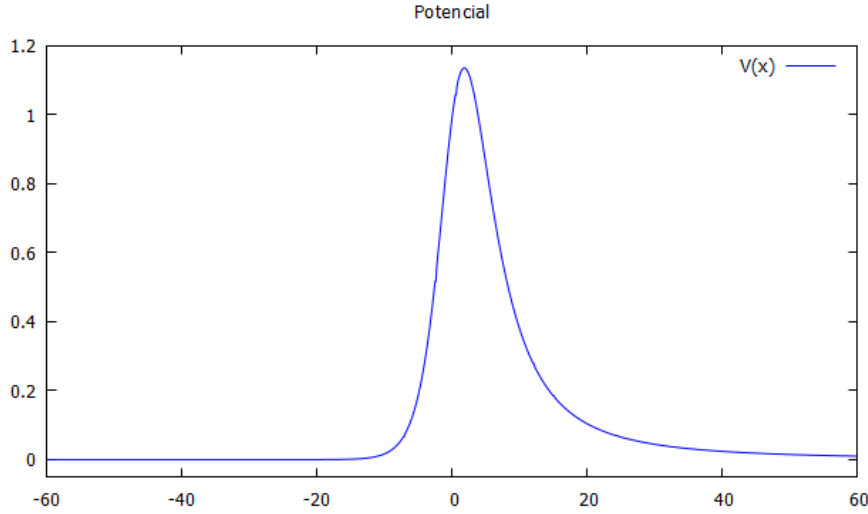


$$\log_{10} |1 - R - T| \text{ Fig. 4.11}$$

Finally we draw σ_l and it has to coincide with Dr Olmo's graphs if we have done all the previous work correctly Fig.4.12.

5.4 Black Bounce: Going from a Schwarzschild BH to a WH.

We are going to go from studying a BH to studying a WH using the same metric but adjusting some parameter. If we change the metric of the equation 2.1 which

Figure 5.9: $V(x)$ 

we will rewrite here for convenience as

$$ds^2 = -A(x)dt^2 + B(x)dx^2 + r^2(x)d\Omega^2$$

with

$$A(x) = B^{-1} = 1 - \frac{r_s}{r(x)} ; \quad r^2(x) = x^2 + a^2$$

as indicated in [32], we can with a simple parameter ‘ a ’ go from studying a BH (values $a < r_s$) to a WH (values $r_s < a < 3M$). That is, we can continuously interpolate between these two ECOs.

In a first approximation, we must be able to reproduce the following graphs of the Schwarzschild BH:

Turtle coordinates, potential, Reflection and Transmission coefficients, transverse absorption spectrum. That is, for BH: $a = 0$ up to $a = 1.5$, we would still be in the behavior domain of a BH.

Since we have changed r^2 we now have

$$x'(y) = 1 - \frac{r_s}{\sqrt[2]{x^2 + a^2}} \quad (5.4)$$

but this time we don’t have an expression that gives us an initial condition, for this we will have to solve first

$$\begin{cases} y'[x] &= \frac{1}{1 - \frac{r_s}{\sqrt[2]{x^2 + a^2}}} \\ y[b] &= b + r_s \cdot \ln(b) - \frac{r_s^2}{b} \end{cases}$$

Figure 5.10: R & T

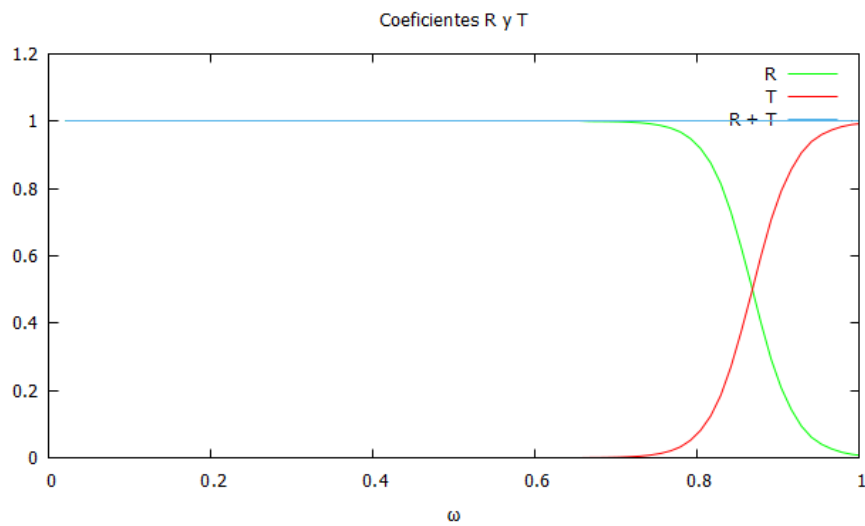
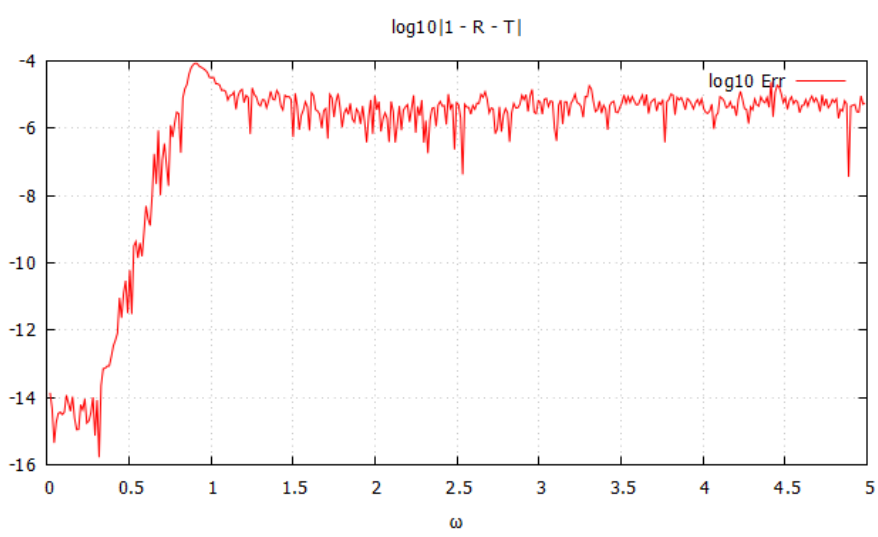
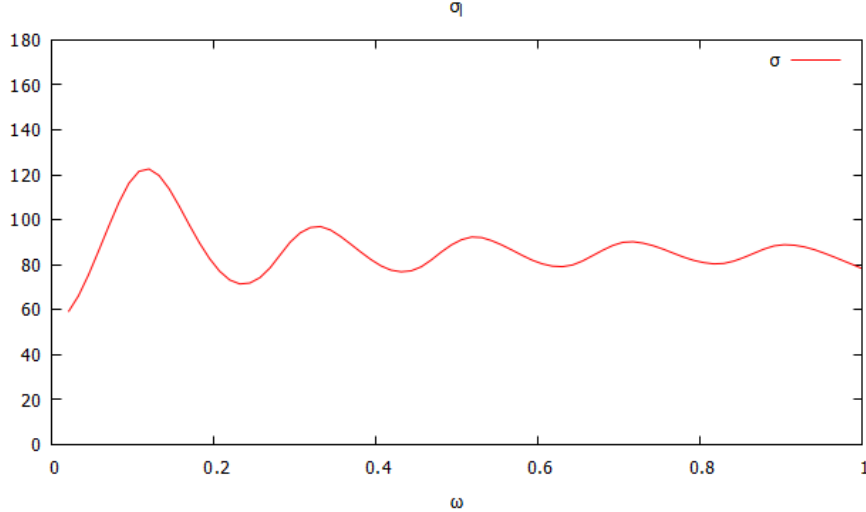
Figure 5.11: $\log_{10}|1 - R - T|$ 

Figure 5.12: σ_l 

when $b \rightarrow +\infty$. Once the initial value problem, PVI, is solved, we already have $y_0 = y[x_0]$, so we can solve the PVI 4.4 when we have x_0 .

The next step is to solve the wave function in the same way that we did in 4.3 but this time the effective potential has the form

$$V_{eff(y,l)} = \frac{l(1+l)A}{r(y)^2} + \frac{r''(y)}{r(y)}$$

where

$$r''(y) = \sqrt[2]{AB} \frac{d(r'(x))}{dx}$$

with which we can now calculate the RT coefficients and in turn obtain the graph of the transverse absorption spectrum. Which, as we can see, exactly matches the expected results. Fig. 4.13 and Fig. 4.15

Now we just have to try to reproduce the behavior of a WH by simply changing our ‘a’ parameter from $a = 0$ to $a = 2.5$. Where we obtain the following graphs Fig. 4.16 - 4.21.

As we see in Fig. 4.16 this time we can pass through the WH, which we could not do in the case of BH. That is, we can go from the positive ordinates to the negative ones. Compare this graph with Fig. 4.7 where not only can we not go to the other side but also our minimum value was r_s .

If we examine the potential Fig. 4.18 we see the two parts of the WH with its two maxima in the different regions of spacetime and its relative minimum in the

Figure 5.13: R & T coefficients

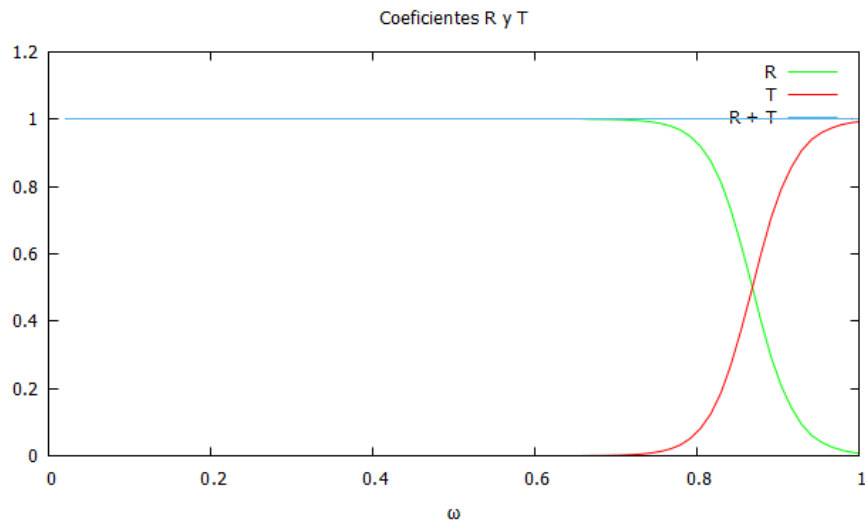
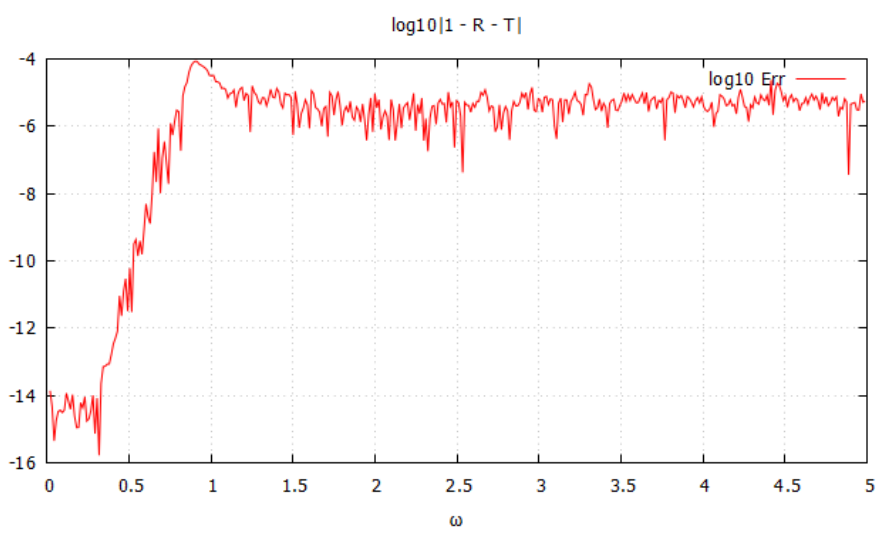
Figure 5.14: $\log_{10}|1 - R - T|$ 

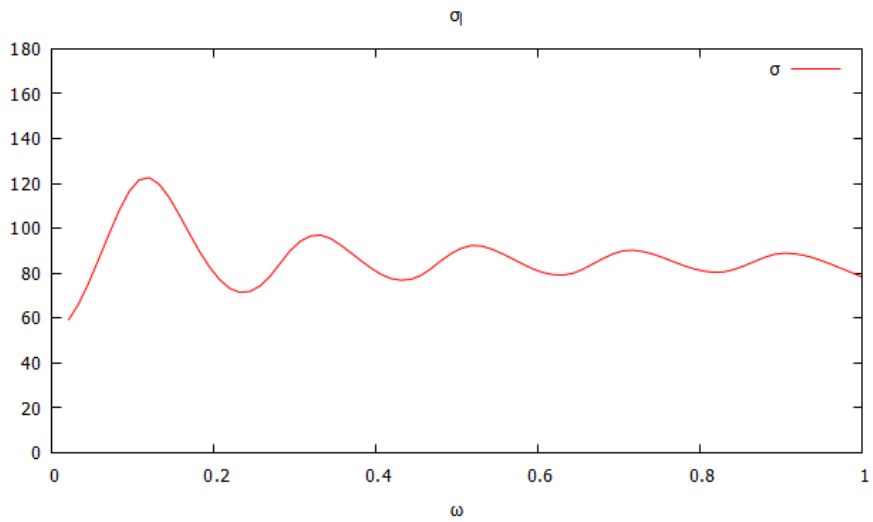
Figure 5.15: σ_l 

Figure 5.16: Turtle

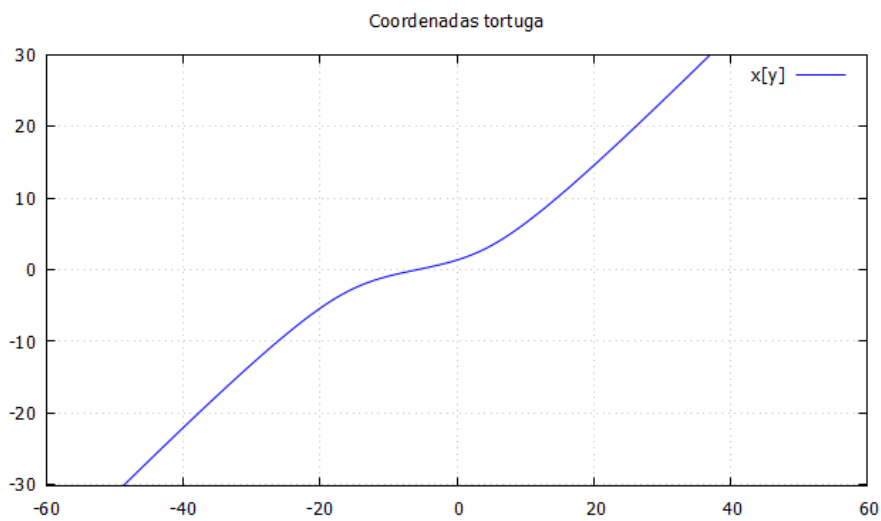


Figure 5.17: Wave and potential

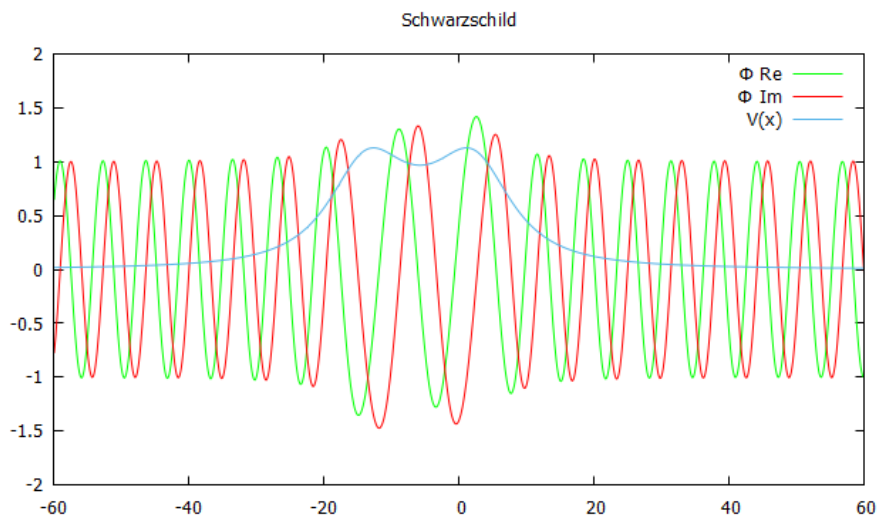
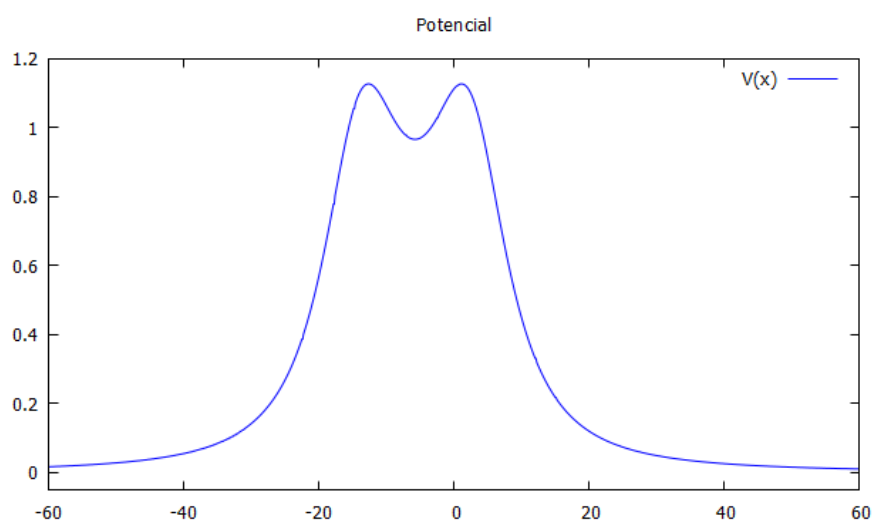
Figure 5.18: $V(x)$ 

Figure 5.19: R & T

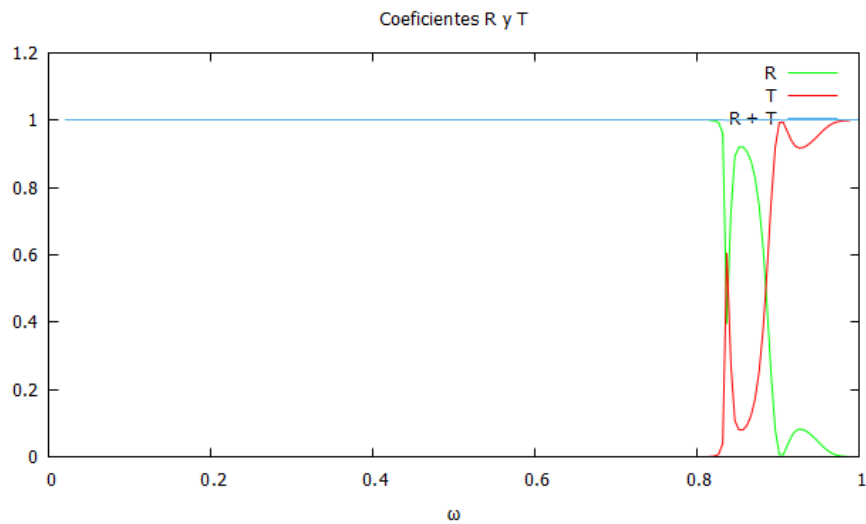
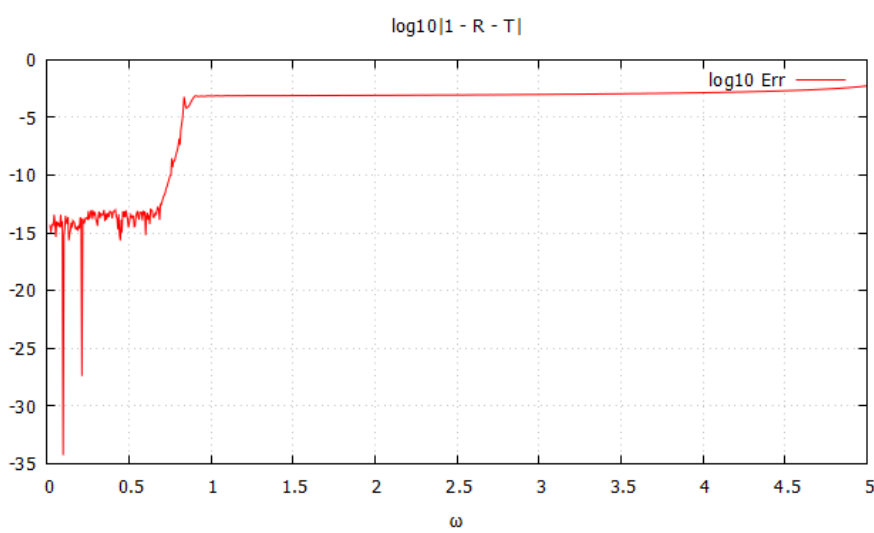
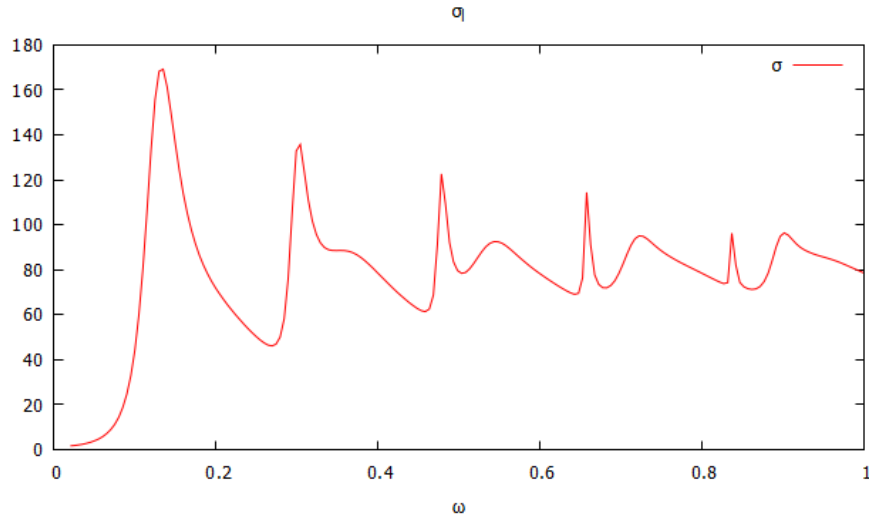
Figure 5.20: σ_l 

Figure 5.21: σ_l 

throat. This plot agrees with Fig. 3 of [9] which is our main reference text.

Fig. 4.19 where we check the coefficients R and T , we also see that it is correct with its sum equal to 1 even though its shape is quite intricate.

In the calculation of the error of the coefficients, its stability around 3 figures is also observed as the frequency increases 4.20

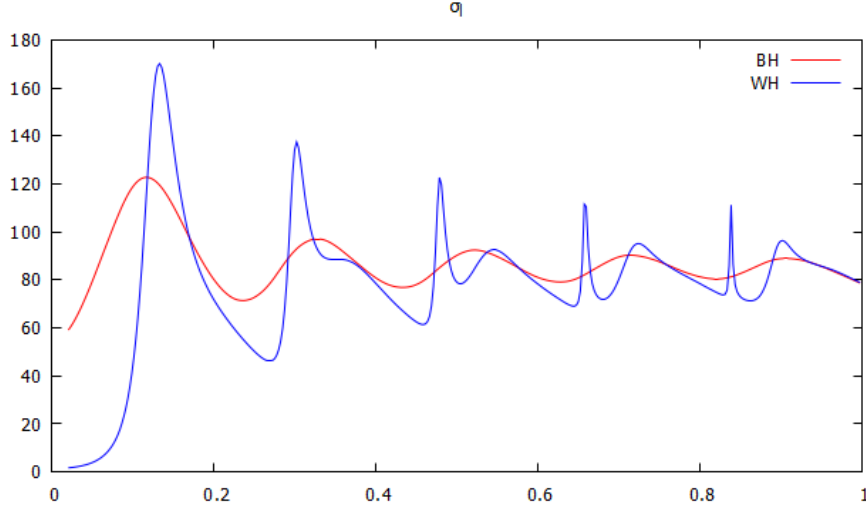
Finally, Fig. 4.21 shows us some resonance peaks that occur in the throat of the WH and clearly this absorption spectrum is different from that of the BH as we obtained in Fig. 4.4, with which we can differentiate a BH from a WH through this type of study. Also this time our figure agrees with Fig. 6 of our reference text [9].

If we unite the graphs of BH and WH we see the difference more clearly Fig. 4.22.

5.5 Scalar wave absorption by thin-membrane wormholes

In this last objective the line element that we are going to work with this time will be

$$ds^2 = -A(x)dt^2 + \frac{1}{A(x)\mathcal{Z}_+^2(x)}dx^2 + r^2(x)(d\theta^2 + \sin^2\theta d\varphi^2)$$

Figure 5.22: σ_l 

where

$$A(x) \equiv \frac{1}{\mathcal{Z}_+(x)} \left[1 - \frac{r_s}{r_c} \frac{(1 + \delta_1 H(x))}{z(x) \mathcal{Z}_-^{1/2}(x)} \right]$$

$$z(x) \equiv \frac{r(x)}{r_c}, \quad \mathcal{Z}_{\pm} \equiv 1 \pm \frac{1}{z^4(x)}$$

$$r^2(x) = 1/2(x^2 + \sqrt{x^2 + 4r_c^2})$$

$$r_c \equiv \sqrt{l_\epsilon r_q}, \quad \delta_1 \equiv \frac{1}{2r_s} \left[\frac{r_q^3}{l_\epsilon} \right]^{1/2}, \quad r_q^2 \equiv 2q^2$$

$$H(x) = -\frac{1}{\delta_c} + 1/2\sqrt{z^4(x) - 1}[f_{3/4}(x) + f_{7/4}(x)]$$

$$f_\lambda(x) = {}_2F_1[1/2, \lambda, 3/2, 1 - z^4(x)]$$

Without a doubt, we are dealing with a much more complicated problem than the previous ones.

A simplification given by the [9] paper is that $\delta_c = \frac{3\Gamma[3/4]^2}{\sqrt{2}\pi^{3/2}}$ approx 0.572069.

We start with the turtle coordinates and that is where our problems begin. We have

$$\begin{cases} x'[y] &= A(y) \mathcal{Z}_+(y) \\ x[+\infty] &= r(y) \end{cases}$$

5.5.1 Hypergeometric

But our program does not work, why? ${}_2F_1$ is the Gaussian hypergeometric function whose definition is

$${}_2F_1(a, b; c; z) = \sum_{n=0}^{\infty} \frac{(a)_n (b)_n}{(c)_n} \frac{z^n}{n!}, |z| < 1; \quad (5.5)$$

So we have a serious problem since our z goes far beyond the unit circle. That's why GSL's *gsl_sf_hyperr_2F1()* function is unable to process $|z| \geq 1$. We start reading references to hypergeometric functions [[35] - [38]] and even find references to tables like Digital Library of Mathematical Functions, DLMF ³ or other useful definitions as in Wolfram ⁴

Even seeing the complexity of the subject, we dare to perform some implementation test using table 13. We implement the (Ec.4.20) of [37] and we see that the results, although correct, are poor.

For example, comparing with Wolfram we have $\text{Hypergeometric2F1}[2., 3., 4., 5.0] = 0.156542 + 0.150796I$ and our result is 0.15625 . With $\text{Hypergeometric2F1}[2., 3., 4., 10.0] = 0.03985 + 0.0188496I$ I get 0.0341796875 . It is clear that we cannot continue down this path as time is running out and the issue is truly complex.

We can't throw in the towel yet. We (vaguely) remember seeing a simplification for this particular case. And we find the answer in (Eq.37) of [10]. We can use a summation. We perform the substitution... but the results are not as expected. Yes, we get turtle coordinates similar to Fig. 4.16 but its shape is not as smooth. We decided to go ahead even though we are not happy at all. We are going to graph the potential that in this case has the form

$$V_{eff}(y, l) = \frac{l(1+l)A(y)}{z^2(y)} + \frac{z''(y)}{z(y)}$$

but the result is horrible. We get the 'ghost shape' as in Fig. 4.18 but it is full of ridges and even the throat is much deeper than it should be. We have reached a dead end, haven't we?

³<https://dlmf.nist.gov/15.8 #E2>

⁴<https://functions.wolfram.com/HypergeometricFunctions/Hypergeometric2F1/02/02/>

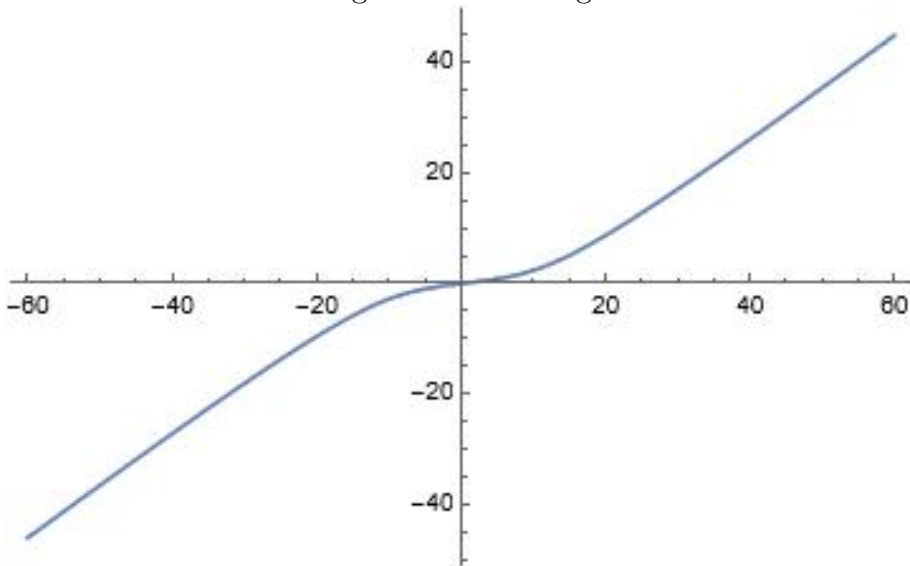
We are out of time but... why not use Wolfram for this last objective if Wolfram handles analytical extensions of hypergeometrics well? Well, there is no other way out. We will have to learn the rudiments of another language in record time.

5.5.2 WolframEngine & Jupyter

Fortunately for us, there is the possibility to use the Wolfram engine for free even with a graphical interface⁵. In my case, and since I did the UNIR Python course, I will use Jupyter for it.

We calculate the turtle coordinates as always, obtaining Fig. 4.23

Figure 5.23: Tortuga

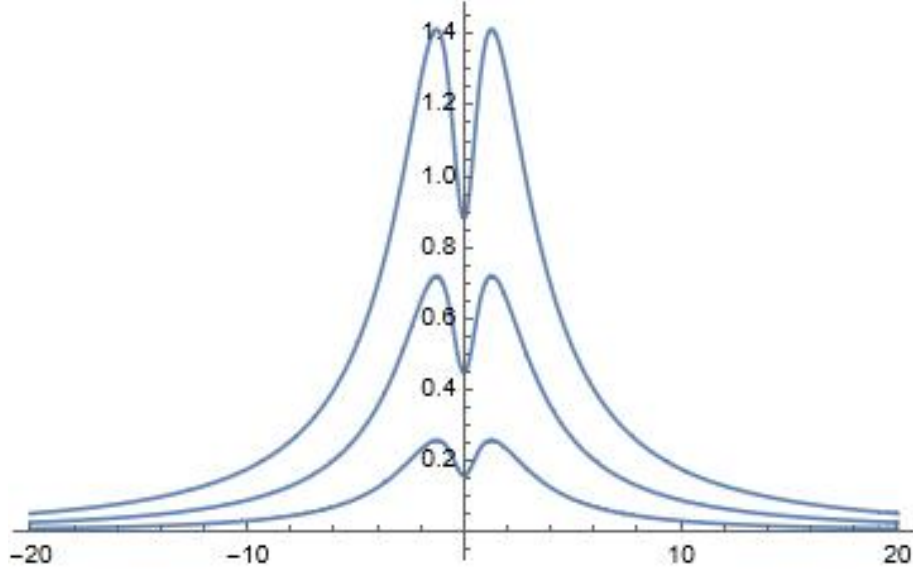


They are perfect. Let us now see the potential for different angular momentum Fig. 4.24

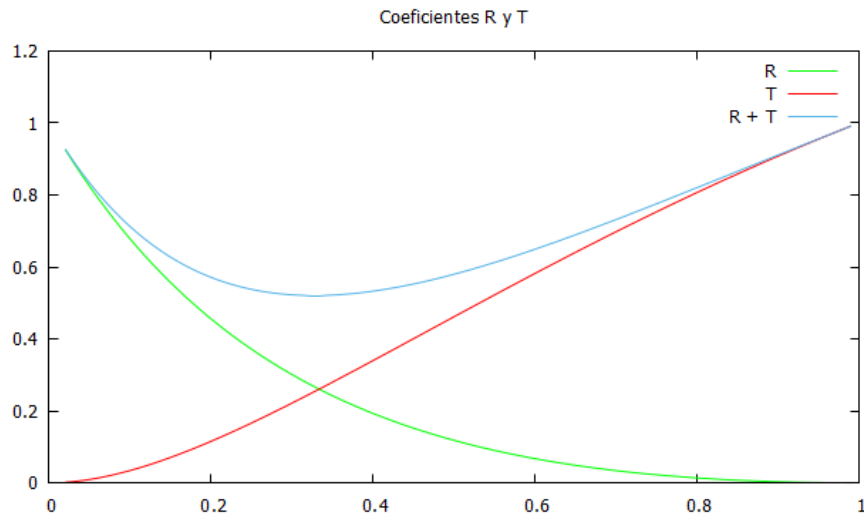
We continue on the right path. Now let's see if we can plot σ_l . No... we are not capable. This is the most complicated part of the code but we have followed our recipe in the same way as in C. We still have time to finish the study so we will not stop until we run out of opportunities.

We say that since it only fails to solve the system of equations when we calculate the waveform, we just need to export the data to a csv file and use it in our C program as we have done before. We do so and evidently the graphs of the turtle

⁵<https://www.wolfram.com/engine/>

Figure 5.24: V_{eff} 

and potential coordinates are exactly the same as those obtained in Wolfram. Now we plot the coefficients R and T to see that everything is fine and we find Fig. 4.25

Figure 5.25: Coeficientes R y T 

Obviously this result is incorrect since we do not have the sum of $R + T = 1$ and therefore we will not be able to graph σ_l . We no longer have more options and we have to finish this MT, which only needs to obtain the graphs of the reflection / transmission coefficients and the absorption spectrum for the case study of the thin membrane wormhole.

This MT has opened before us a whole ocean of new things to learn since we

have discovered for ourselves the hypergeometric functions and their importance. We have also discovered that differential equations can be solved using power series. We have realized that we can carry out all series of physical experiments from home with our computer and that these experiments can be interactive. For example, with the equations of motion of a pendulum, we can draw and animate it by making it follow the laws of physics (which would be a rudimentary physics engine in a game). And all this thanks to the numerical methods and the bases that we have studied in the master's degree.

Chapter 6

Conclusions and Future Work

We have seen that it is possible to differentiate between a BH and a WH by means of the scalar wave absorption technique on theoretical models, therefore in the future all this knowledge can be used so that when we obtain information from an ECHO we can characterize it. This could also lead in the future to rule out, in principle, certain current models or ideas about gravitation.

We also see that we have obtained 2 of our 3 specific objectives, obtaining the absorption spectrum using scalar waves of:

1. A Schwarzschild black hole
2. A wormhole using Black Bounce geometry

only pending is the acquisition of the absorption spectrum in the case of the thin membrane wormhole

The first pending task is clearly to obtain σ_l using the program written in Wolfram, that is, to fulfill our third objective. It is clear that the solution is there, only that it has eluded us. A deeper understanding of the language is necessary to see where the error is.

Undoubtedly one of the pending tasks left by this MT is the integration of the Numerov algorithm in the GSL API because historically it is the method that has been used to solve everything that has to do with the Schrödinger equation and it seems natural to solve these problems also by this numerical method.

Also, in connection with this work, some way of carrying out and handling in a simple way the analytical extension of the Gaussian hypergeometric is necessary, but it is clear that a deep understanding of the function is needed and not a superficial one as we have right now. Perhaps explore the arbitrary precision ball arithmetic library, Arb¹ as it looks promising.

¹<https://arblib.org/>

Bibliography

- [1] B. P. Abbott *et al.* [LIGO Scientific and Virgo], *Observation of Gravitational Waves from a Binary Black Hole Merger*, Phys. Rev. Lett. 116 (2016) 061102. This publication echoes the observational results obtained by LIGO.
- [2] B. P. Abbott *et al.* [LIGO Scientific and Virgo], *GW170817: Observation of Gravitational Waves from a Binary Neutron Star Inspiral*, Phys. Rev. Lett. 119 (2017) 161101. Publication that reveals the results of the observation of gravitational waves produced by a pair of neutron stars in spiral rotation.
- [3] K. Akiyama *et al.* [Event Horizon Telescope], *First M87 Event Horizon Telescope Results. I. The Shadow of the Supermassive Black Hole*, Astrophys. J. Lett. 875 (2019) L1. This article refers to the different techniques used to obtain the first image of an ECO.
- [4] V. Cardoso and P. Pani, *Testing the nature of dark compact objects: a status report*, Living Rev. Rel. 22 (2019) 4. This paper deals with the nature of different ECOs and how their understanding will allow physics to go further.
- [5] M. Visser, *Lorentzian wormholes* (Springer-Verlag, New York, 1996). This book pushes physics theories to their limits and deduces the physics of exotic objects like wormholes.
- [6] A. Einstein and N. Rosen, Phys. Rev. 48, 73 (1935). This article of only 5 sheets mentions the possibility of a 'bridge' between two sheets of space: a traversable wormhole.

- [7] F. S. N. Lobo, G. J. Olmo, E. Orazi, D. Rubiera-Garcia and A. Rustam, *Structure and stability of traversable thin-shell wormholes in Palatini $f(\mathcal{R})$ gravity*, Phys. Rev. D 102, no.10, 104012 (2020) doi:10.1103/PhysRevD.102.104012 [arXiv:2009.10997 [gr-qc]]. This article studies the structure and stability of thin-membrane wormholes.
- [8] LIGO SCIENTIFIC COLLABORATION, *An improved analysis of GW150914 using a fully spin-precessing waveform model* arXiv:1606.01210 [gr-qc] 10.1103/PhysRevX.6.041014 The data of the GW150914 of the shock of a binary black hole obtained by LIGO are studied
- [9] ADRIA DELHOM, CAIO F. B. MACEDO, GONZALO J. OLMO, LUÍS C. B. CRISPINO (2019), *Absorption by black hole remnants in metric-affine gravity*. arXiv:1906.06411v1 [gr-qc] DOI 10.1103/PhysRevD.100.024016 Using numerical methods, the absorption properties of a family of non-singular solutions are investigated. The spectrum obtained is characterized by a series of quasi-bound states of excitation, associated with the existence of a photostable sphere.
- [10] GONZALO J. OLMO1, D. RUBIERA-GARCIA, *Reissner-Nordström Black Holes in Extended Palatini Theories* arXiv:1207.6004v1 [gr-qc] DOI 10.1103/PhysRevD.86.044014 In this paper, spherically symmetric static solutions with an electric field are studied.
- [11] MERCE GUERRERO, GONZALO J. OLMO, DIEGO RUBIERA-GARCIA, Y DIEGO SÁEZ-CHILLÓN GÓMEZ, *Shadows and optical appearance of black bounces illuminated by a thin accretion disk* arXiv:2105.15073v2 [gr-qc] DOI 10.1088/1475-7516/2021/08/036 In which the light and shadow rings of a family of symmetric spherical geometries are studied by interpolating between a Schwarzschild solution, a typical black hole, and a traversable wormhole.
- [12] OLIVER JAMES, EUGÉNIE VON TUNZELMANN, PAUL FRANKLIN, KIP S THORNE (2015), *Gravitational Lensing by Spinning Black Holes in Astrophysics, and in the Movie Interstellar* arXiv:1502.03808v2 [gr-qc] DOI

10.1088/0264-9381/32/6/065001 This article describes Hollywood's effort to rigorously characterize what a black hole might look like.

- [13] ROBERT GEROCH, *What is a singularity in general relativity?* DOI 10.1016/0003-4916(68)90144-9 Here the intuitive passage from singularity as "something that becomes infinite" to the notion of geodesic completeness is explained by means of examples.
- [14] ABBAS ASKAR, KRZYSZTOF BELCZYNSKI, GIANFRANCO BERTONE..., *Black holes, gravitational waves and fundamental physics: a roadmap* This is a very long paper of 217 pages in which aspects of black holes, gravitational waves...
- [15] ELISA MAGGIO, PAOLO PANI, VALERIA FERRARI (2017), *Exotic Compact Objects and How to Quench their Ergoregion Instability* arXiv:1703.03696v3 [gr-qc] DOI 10.1103/PhysRevD.96.104047 Gravitational waves give us access to the structures of black holes. A simple perturbation model in Kerr geometry with a reflective surface near the horizon is investigated.
- [16] EMANUELE BERTI¹, VITOR CARDOSO¹, ANDREI O. STARINETS (2009), *Quasinormal modes of black holes and black branes* arXiv:0905.2975v2 [gr-qc] DOI 10.1088/0264-9381/26/16/163001 This is an extensive article gathering information on quasinormal modes in black holes and black branes.
- [17] ALEXANDRE ARBEY, JÉRÉMY AUFGINGER (2020), *BlackHawk: A public code for calculating the Hawking evaporation spectra of any black hole distribution* arXiv:1905.04268v2 [gr-qc] DOI 10.1140/epjc/s10052-019-7161-1 This paper describes a C code (there is also code in Mathematica) among others about the distribution in black holes and also talks about the problems they have found when performing the numerical simulations.
- [18] SÉRGIO L. MORELHÃO, ANDRÉ V. PERROTTA, *General recursive solution for one dimensional quantum potentials: a simple tool for applied physics* (2007) arXiv:quant-ph/0605115 This article reviews a simplified version of the computation of wavefunctions in a 1-dimensional potential.

- [19] KARL MARTEL, ERIC POISSON, *Regular coordinate systems for Schwarzschild and other spherical spacetimes* (2000) arXiv:gr-qc/0001069 This article intends to introduce new coordinate systems, but initially talks about Eddington-Finkelstein coordinates.
- [20] PER KRAUS, FRANK WILCZEK, *A Simple Stationary Line Element for the Schwarzschild Geometry, and Some Applications* (1994) arXiv:gr-qc/0001069 This article talks about turtle coordinates and Reissner-Nordstrom geometry (which will be important to deal with WH) among others.
- [21] JUN REN, ZHENG ZHAO, *Hawking Radiation via Tunnelling from Black Holes by Using Eddington–Finkelstein Coordinates* (2006) DOI: 10.1007/s10773-006-9101-8 The article deals with the tunneling effect of BBHs using turtle coordinates.
- [22] MATTHIAS TROYER (2012), *The quantum one-body problem. Chapter 03 Computational Quantum Physics* <https://edu.itp.phys.ethz.ch/fs12/cqp/> FS 2012 Where the time-independent 1-dimensional equation of the Schrödinger equation is treated.
- [23] SÉRGIO L. MORELHÃO1 ANDRÉ V. PERROTTA, *General recursive solution for one-dimensional quantum potentials: a simple tool for applied physics* Revista Brasileira de Ensino de Física, v. 29, n. 3, p. 331-339, (2007) www.sbfisica.org.br This article describes simplified equations for computing one-dimensional wave equations given a potential using Numerov's method.
- [24] TAO PANG (2006), *An Introduction to Computational Physics. Ed. Cambridge* This book deals with different numerical methods directly applied to physical problems.
- [25] R. FABBRI (1975), *Scattering and absorption of electromagnetic waves by a Schwarzschild black hole* Phys. Rev. D 12, 933 DOI <https://doi.org/10.1103/PhysRevD.12.933> The article deals with the scattering and absorption of electromagnetic waves by a non-rotating symmetric

black hole in the Schwarzschild background, and shows that a black hole is not capable of absorbing electromagnetic waves when the wavelength of the radiation is greater than the Schwarzschild radius.

- [26] TH LALOYAUX, PH LAMBIN, J.-P VIGNERON, A.A LUCAS (1989), *Resolution of the one-dimensional scattering problem by a finite element method* Journal of Computational Physics, Volume 83, Issue 2 DOI [https://doi.org/10.1016/0021-9991\(89\)90126-5](https://doi.org/10.1016/0021-9991(89)90126-5) The article deals with the finite element method to obtain the tunneling scattering solutions of the 1-dimensional Schrödinger equation.
- [27] NORTON, M. (2009), *Numerov's Method for Approximating Solutions to Poisson's Equation*. <https://www.siue.edu/~mnorton/Numerov.pdf> Article where a brief summary of different numerical methods is made using the Poisson equation as an excuse. The methods used in the comparison are: Euler, Euler-Cromer, Feynman-Newton and Numerov.
- [28] JOHN M BLATT (1967), *Practical points concerning the solution of the Schrödinger equation* Journal of Computational Physics, Volume 1, Issue 3; DOI [https://doi.org/10.1016/0021-9991\(67\)90046-0](https://doi.org/10.1016/0021-9991(67)90046-0) In the article numerical solutions to the one-dimensional Schrödinger equation using Numerov are considered and some useful tips on their use are given.
- [29] MERCE GUERRERO, GONZALO J. OLMO, Y AND DIEGO RUBIERA-GARCIA (2021), *Double shadows of reflection-asymmetric wormholes supported by positive energy thin-shells* arXiv:2102.00840 [gr-qc] DOI 10.1088/1475-7516/2021/04/066 Article that deals with one of the characteristics that differentiates wormholes from black holes: their shadow. Specifically, we speak of double-shadowed wormholes.
- [30] T.E.SIMOS, P.S.WILLIANS (1997), *A family of Numerov-type exponentially fitted methods for the numerical integration of the Schrödinger equation* 10.1016/0377-0427(94)00126-X Article dealing with different Numerov-type

predictor-corrector methods. In it he realizes that the global order of the algorithm is $O(4)$ but it is still usually better than other algorithms of the same order..

- [31] PABLO BUENO, PABLO A. CANO, FREDERIK GOELEN, THOMAS HERTOG, BERT VERCNOCKE, *Echoes of Kerr-like wormholes* DOI <https://doi.org/10.1103/PhysRevD.97.024040> Study on ECOs thanks to gravitational waves.
- [32] MERCE GUERRERO, GONZALO J. OLMO, DIEGO RUBIERA-GARCIA, DIEGO SÁEZ-CHILLÓN GÓMEZ, *Shadows and optical appearance of black bounces illuminated by a thin accretion disk* arXiv:2105.15073v2 [gr-qc] DOI 10.1088/1475-7516/2021/08/036 I work on the shadows and light rays that black holes and wormholes would have. Black Bounces are used to smoothly pass between BH and WH.
- [33] MIGUEL ALCUBIERRE, FRANCISCO S. N. LOBO, *Warp drive basics* arXiv:2103.05610v1 [gr-qc] DOI 10.1007/978-3-319-55182-1 Basic fundamentals of the Alcubierre engine
- [34] MICHAEL S. MORRIS, KIP S. THORNE, *Wormholes in spacetime and their use for interstellar travel: A tool for teaching general relativity* DOI 10.1119/1.15620 It uses the possibility of using wormholes to travel in spacetime as a way to teach general relativity in an elementary way.
- [35] W.BECKEN, P.SCHMELCHER, *The analytic continuation of the Gaussian hypergeometric function ${}_2F_1(a,b;c;z)$ for arbitrary parameters* DOI 10.1016/S0377-0427(00)00267-3 Shows a complete table of formulas for the analytic continuation of the hypergeometric function.
- [36] ROBERT C.FORREY, *Computing the Hypergeometric Function* DOI 10.1006/jcph.1997.5794 Explain how to compute the real variable hypergeometric for arbitrary real parameters.

- [37] JOHN PEARSON, WORCESTER COLLEGE, *Computation of Hypergeometric Functions* It gives some tables and guidelines to calculate the hypergeometric for different parameters in the complex plane.
- [38] GEORGE E. ANDREWS, *Problems and Prospects for Basic Hypergeometric Functions* DOI 10.1016/B978-0-12-064850-4.50008-2 Analyzes certain problems and perspectives of the basic hypergeometric functions.

Chapter 7

Glosario

LIGO Laser Interferometer Gravitational-Wave Observatory

VIRGO European interferometer named for the constellation Virgo (played on the similar word LIGO)

BH Black Hole

WH Worm Hole

Veritasium www.youtube.com/c/veritasium

ECO Extreme / Exotic Compact Objects

UCO Ultra-Compact Objects

ClePhOs Clean Photonsphere Objects

GW Gravitational Waves

Brana Extended object with any number of dimensions in which a string in string theory is an example of dimension one. **GSL** GNU Scientific Library, www.gnu.org/software/gsl

GNUpot GNU Plot, gnuplot.info

GMP GMP, gmplib.org

GLib GLib, gitlab.gnome.org/GNOME/glib

TCL Tool Command Language, www.tcl.tk

LISA Laser Interferometer Space Antenna

ESA European Space Agency

LPF LISA PathFinder

Wolfram Wolfram, wolfram.com

Appendix A

Appendices

A.1 Source code

The source code of this MT can be found in the repository of GitHub